

August 2014

Experimental, Numerical and Analytical Characterization of Torsional Disk Coupling Systems

Alex B. Francis

University of Wisconsin-Milwaukee

Follow this and additional works at: <https://dc.uwm.edu/etd>

 Part of the [Mechanical Engineering Commons](#)

Recommended Citation

Francis, Alex B., "Experimental, Numerical and Analytical Characterization of Torsional Disk Coupling Systems" (2014). *Theses and Dissertations*. 625.

<https://dc.uwm.edu/etd/625>

This Thesis is brought to you for free and open access by UWM Digital Commons. It has been accepted for inclusion in Theses and Dissertations by an authorized administrator of UWM Digital Commons. For more information, please contact open-access@uwm.edu.

**EXPERIMENTAL, NUMERICAL AND ANALYTICAL
CHARACTERIZATION OF TORSIONAL DISK COUPLING SYSTEMS**

by

Alex Francis

A Thesis Submitted in
Partial Fulfillment of the
Requirements for the Degree of

Master of Science
in Engineering

at

The University of Wisconsin-Milwaukee

August 2014

ABSTRACT

EXPERIMENTAL, NUMERICAL AND ANALYTICAL CHARACTERIZATION OF TORSIONAL DISK COUPLING SYSTEMS

by

Alex Francis

The University of Wisconsin-Milwaukee, 2014
Under the Supervision of Professor Ilya Avdeev

Torsional couplings are used to transmit power between rotating components in various power systems while allowing for small amounts of misalignment that may otherwise lead to equipment failure. When selecting a proper coupling type and size, one has to consider three important conditions: (1) the maximum load applied to the coupling, (2) the maximum operation speed, and (3) the amount of misalignment allowable for normal operation. There are many types of flexible couplings that use various materials for the flexible element of the coupling. The design of the coupling and the materials used for the flexible portion will determine its operating characteristics. In this project, investigation of a disk coupling that uses a stack of metallic discs to counter the misalignment effects is performed. Benefits of this type of coupling include: ease of replacement or repair, clear visual feedback of element failure, and the absence of a need for lubrication. The torsional stiffness of a coupling is a major factor relative to the amount of misalignment allowable. Currently, flexible couplings are tested by manufacturers to experimentally determine the torsional stiffness; a process which requires expensive equipment and more importantly employee time to set-up and run. The torsional coupling lumped characteristics, such as torsional- and flexural stiffness, as well as natural frequencies are important for design of the entire power system and have

to be as precise as possible. In this work, we have developed an accurate modeling framework for determining these parameters based on a full 3-D finite element model and model-order reduction procedure. Developed methodology was validated by available experimental data from a regional manufacturer of torsional couplings.

© Copyright by Alex Francis, 2014
All rights Reserved

Dedicated to the perpetual support of my family, friends and faculty mentors;
with special thanks to my Grandfather, John F. Francis, whose influential passion for engineering
and keen interest in the way things work has encouraged me throughout my studies.

TABLE OF CONTENTS

Table of Contents.....	vi
List of Figures.....	viii
List of Tables	x
Acknowledgments.....	xi
1. Introduction.....	1
1.1. History and Applications of Torsional Couplings	1
1.2. Design Considerations	1
1.3. State-of-the-Art in Torsional Couplings Modeling.....	3
1.4. Motivation for Reduced Order Modeling	4
2. Review of Model Order Reduction Techniques for Structural Analysis.....	6
2.1. ROM Overview.....	6
2.2. Relevant Applications	6
3. Analytical Model of a Torsional Disk Coupling System.....	9
3.1. Assumptions.....	9
3.2. Torsional Stiffness	9
3.3. Misalignment Stiffness	14
4. Full 3-D Numerical Model of a Torsional Disk Coupling System.....	16
4.1. Geometry Considerations.....	16
4.2. Material Selection and Assumptions.....	18
4.3. Modeling Flexible Disk Pack - Contact Analysis.....	21
4.4. Eigenvalue Analysis - Natural Modes of Vibration.....	28
4.5. Steady State Static Analysis - Torsional and Bending Stiffness.....	34
5. Reduced-order Model of a Torsional Disk Coupling System.....	44
5.1. Model-order Reduction Approach	44
5.2. Results.....	46
6. Experimental Validation.....	49

6.1. Experimental Setup and Results	49
6.2. Comparison of Analytical, Reduced-order and Full Models	51
7. Summary of Results.....	54
7.1. Conclusions.....	54
7.2. Contributions.....	55
7.3. Future Work.....	56
References.....	57i

LIST OF FIGURES

Figure 2.1: Example power system vibration model with simplified stiffness components [8].....	7
Figure 2.2: Example power system vibration model with simplified stiffness components [19].....	8
Figure 3.1: a) Hooke's Joint representation b) Pinned-joint representation [8]	10
Figure 3.2: Coupling system schematic a) coupling in system b) free-body diagram [59],[10]	11
Figure 3.3: Example rigid coupling representation [59].....	11
Figure 3.4: Theoretical representation of flexible disc coupling	12
Figure 4.1: 3D Solidworks model of flexible disc coupling.....	17
Figure 4.2: ANSYS Automatic script procedure	18
Figure 4.3: Diagram comparing the change in material properties of each component	20
Figure 4.4: Influence of disc pack thickness on K_T	22
Figure 4.5: a) isolated disc pack section (top view) b) disc pack model (side view)	23
Figure 4.6: ANSYS disc pack model deformed state (3-disc layers)	24
Figure 4.7: : a) Beam constraints b) Timoshenko standard beam model [67].....	25
Figure 4.8: Disc pack FE model comparison a) multiple discs b) solid disc pack	27
Figure 4.9: Lateral Modes: a) Mode 8 - Bending and b) Mode 9 – Tension	31
Figure 4.10: Center Member mode shapes: a) Mode 11 - Wobble and b) Mode 13 – Translation	32
Figure 4.11: a) Mode 12 – Disc Flexure and b) Mode 14 – Flywheel Adapter Flexure.....	33
Figure 4.12: Mode 15 – Torsional Frequency	34
Figure 4.13: a) Method 1 geometry b) Method 1 loads and constraints	36
Figure 4.14: a) Method 2 geometry b) Method 2 loads and constraints	38
Figure 4.15: ANSYS Method 1 simulation result a) Von Mises stress b) Displacement sum	40
Figure 4.16: Simplified ANSYS representation	41
Figure 5.1: ANSYS ROM procedure.....	44
Figure 5.2: ROM model Master DOF.....	45

Figure 5.3: ROM mode #7 stress contour a) entire coupling b) isolated disc pack	47
Figure 5.4: ROM superelement example capabilities	48
Figure 6.1: Experimental Set-up and Indicator Placements [Rexnord]	49
Figure 6.2: Simulated shaft constraints and loads	52

LIST OF TABLES

Table 1.1: Categories of flexible coupling designs.....	2
Table 3.1: Overview of shaft misalignment types [60].....	14
Table 4.1: Component Material Properties.....	19
Table 4.2: Material property study results Summary.....	20
Table 4.3: Disc pack thickness data and deviation from the original value	22
Table 4.4: Shear modulus comparison.....	28
Table 4.5: Summary of Mode Shapes and Results	29
Table 4.6: Method vs Torsional Stiffness	41
Table 4.7: Theoretical torsional stiffness result accuracy.....	42
Table 4.8: Shaft parallel misalignment stiffness.....	42
Table 6.1: Comparison of simulation results with experimental results.....	51
Table 6.2: Theoretical shaft parameters.....	52
Table 6.3: Comparison of theoretical and simulation shaft results.....	53

ACKNOWLEDGMENTS

I would like to thank my advisor, Dr. Ilya Avdeev, whose guidance has been critical to successful research projects in the Advanced Manufacturing and Design Lab. I also would like to thank the industry partner of this project, Rexnord, and key personnel driving the research initiative, Sundar Ananthasivan and Dr. Joseph Hamann. Additional thanks to Dr. Hamann and Dr. Anoop Dhingra for serving on my thesis committee and offering valuable feedback.

The support from members of our lab, Mir Shams and Mehdi Gilaki, has also been of immense assistance which must not go unnoticed. Finally, I am grateful for the support of my parents, family, and friends through this journey inside and outside academics.

1. Introduction

1.1. History and Applications of Torsional Couplings

Power systems, such as generators, pumps, and turbomachinery with rotating components often incorporate coupled shafts to transmit power throughout the system. There are generally two types of coupling devices: rigid and flexible [1]. Historically, rigid flanges were used as the coupling member and are still used in some circumstances. Consequently, as the performance of power systems became more critical, these rigid members failed to offer adequate tolerance for misalignments. Flexible couplings are now used to transmit power between rotating components in various power systems, while allowing for relatively small misalignment that may otherwise lead to equipment failure.

Couplings are often the least expensive component of a rotating system but protect the most expensive and valuable components when they are designed to break before transmitting harmful forces through the system [2]. Applications of mechanical couplings include power plant generator systems, manufacturing facilities, and mining industry conveyors. For example, in the mining industry, a day of lost production time could result in millions of lost revenue [3].

1.2. Design Considerations

The flexible disc couplings were invented by M.T. Thomas in 1919. The original design used a pack of thin metal discs, which would flex to account for any misalignments [4]. Advantages of the flexible disc couplings are: a near infinite lifetime,

relative ease of visually inspect and quickest replacement time with a low labor cost [2], [5].

“In coupling applications, misalignment is the rule rather than the exception” [6].

Since the introduction of the original flexible metallic disk coupling there have been variations on the flexible coupling design; various flexible coupling categories are compared in Table 1.1 [2], [5], [6], [7].

Table 1.1: Categories of flexible coupling designs

Coupling Type	Application Speed	Application Torque	Misalignment*
Sliding Disk	Low	High	½° Angular 0.25" Parallel Shaft-Centerline
Gear	Low-High	High	1-3° Angular
Roller Chain	Low-High	High	1.5° Angular 0.010" Parallel Shaft-Centerline
Spring	Low-High	Low	4° Angular 0.25" Parallel Shaft-Centerline
Flexible Disk	Low	High	1° Angular
	High	Low	0.0625" Parallel Shaft-Centerline
Bellows	Low	Low	9° Angular 0.25" Parallel Shaft-Centerline
Elastomeric Sleeve	Low-High	Low	1° Angular 0.062" Parallel Shaft-Centerline
Bonded Elastomeric Disk	Low	Low	4° Angular
Rubber Cap	Low	High	1° Angular 0.25" Parallel Shaft-Centerline

*Varies by manufacturer, coupling size, and flexible element material selection.

Flexible couplings are designed to transmit torque smoothly, while accommodating for axial, radial, or angular misalignments [1]. When selecting a coupling, an engineer would refer to manufacturer's catalogs and available data rather than designing a one from the ground up [6]. One of the most important design requirements for shaft couplings is absence of slip while transmitting shaft torque. It is also important for the coupling to not exhibit premature failure with respect to other components in the system [6].

1.3. State-of-the-Art in Torsional Couplings Modeling

There is a substantial body of literature investigating industrial rigid couplings in turbomachinery focused on modeling, analysis techniques, and types of failure [7], [9], [10], [11], [12], [13], [14]. In addition, there are many text books available describing rotor systems and power dynamics [9], [15], [16], [17], [18], [19].

In the presence of misalignments the coupling can induce static and dynamic forces on the rest of the system, which can result in damage to machinery components, such as bearings, shafts, and even the coupling itself [8]. Vibration response of the system is another set of design parameters that must be taken into account.

Vibration modeling ranges from eigenvalue analysis of full system modeling to specific studies of individual components. Discussion of vibration modeling and numerical simulations of drive systems can be found in [20], [21], [22], [23], [24], [25], [26]. Specific investigation of torsional vibration can be found in [27], [28],[29]. Torsional stiffness is a key factor when studying torsional vibrations and some authors have conducted torsional stiffness studies of gears, shafts, and even shaft connections

[30], [31], [32]. Sheikh has explored numerical finite element methods to study rigid-type coupling systems [33], while Kahraman and his colleagues investigated the dynamics of geared rotors [34]. There are only few studies related to the design of metallic flexible disc couplings specific to the flexible membrane coupling, which is similar to the flexible disc coupling [35].

Ovalle studied the effect of misalignment on systems using flexible disc coupling CAD models and numerical FE simulations [36]. Other authors have investigated coupling misalignment forces on the system [37], [38], [39], [40].

The nature of excitation forces and torsional vibration can lead to undetectable deformation modes that can lead to failure. Redmond identified misalignment as a source of vibration and the lack of investigative work in the area [8]. Tadeo also noted that there was a lack of information about the forces and bending moments generated in the coupling due to misalignment, which hinders the understanding of how the coupling influences the system [41].

In summary, there are many investigations of rigid and gear couplings as well as power systems for both static and vibration analysis but there is an evident lack of research specific to flexible disc couplings.

1.4. Motivation for Reduced Order Modeling

The ambition of this study is to create a multi level engineering tool for increased understanding of the flexible disc coupling and various applications. Specifically, for torsional stiffness calculation/understanding, modal frequency analysis, and reduced

order modeling for use of this information in a larger system level design study. Specific to flexible disc coupling systems, the disc pack is a multi-layer stack of discs which becomes complex when conducting finite element analysis due to the necessity for added non-linear contact elements. Reduced-order models have been used to drastically reduce the computational cost of numerical simulations while maintaining sufficient accuracy. A comprehensive review of model reduction methods through the late 1980s can be found in work by Villemagne [42]. In all, the flexible disc coupling analysis tool will be a finite element based modeling scheme with verification by theoretical, analytical, and experimental studies.

2. Review of Model Order Reduction Techniques for Structural Analysis

2.1. ROM Overview

The interest of reduced order modeling (ROM) techniques spawned from a need for efficient numerical techniques when simulating large-scale systems. Applications of reduced order modeling span from large and complex models in structural dynamics such as gas turbine systems down to circuit simulation and even microelectromechanical (MEMS) system simulation [43], [44], [45], [46], [47] as well as in fields of and not limited to fluid dynamics, biological systems, neuroscience, chemical engineering and mechanical engineering [48], [49]. The analytical technique of ROM is an efficient tool to replace large models with an approximate smaller model that captures dynamical behavior and preserves essential properties [43]. Additionally, ROM is a very computationally friendly way of solving complex non-linear systems [50].

2.2. Relevant Applications

In power system dynamics, the ROM was used to simplify complex rotating equipment [51], [52], [53], [54], [55]. Typically, engineers would simplify the dynamic drive system by converting components to a series of springs and dampers; Figure 2.1 and Figure 2.2 show examples of a system model. For example, the flexible coupling element can be simplified into stiffness components that react to torsional loads and lateral misalignments in the system. The methods of simplification are discussed later in Section 5. A better understanding of the coupling itself can prevent unintended failure of expensive drive components or motors and prolong the life of the entire system. Thus, a computational model of the flexible coupling can be used as a resource for analysis of

modes or the stiffness properties in various degrees of freedom. When each component of the flexible coupling is modeled in detail, the computational model can become quite large. Using ROM techniques can yield a more efficient design process for studying properties of flexible couplings.

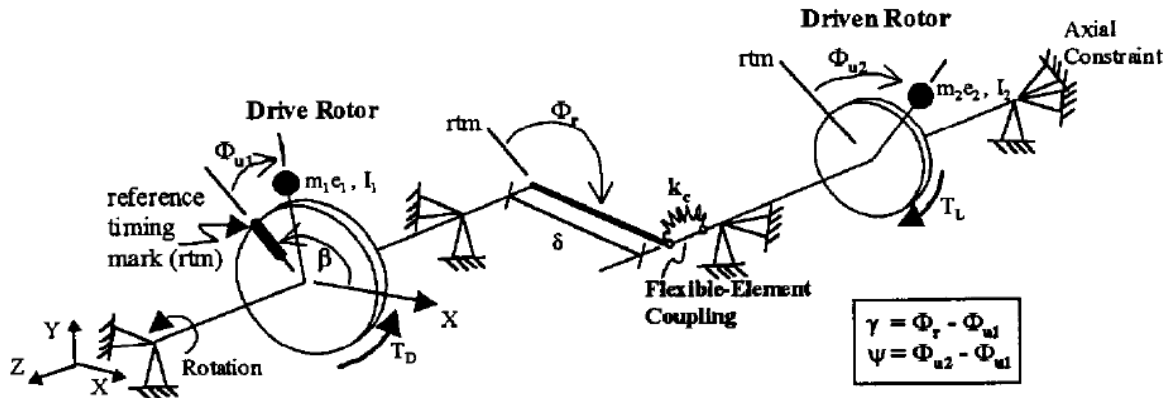


Figure 2.1: Example power system vibration model with simplified stiffness components [8]

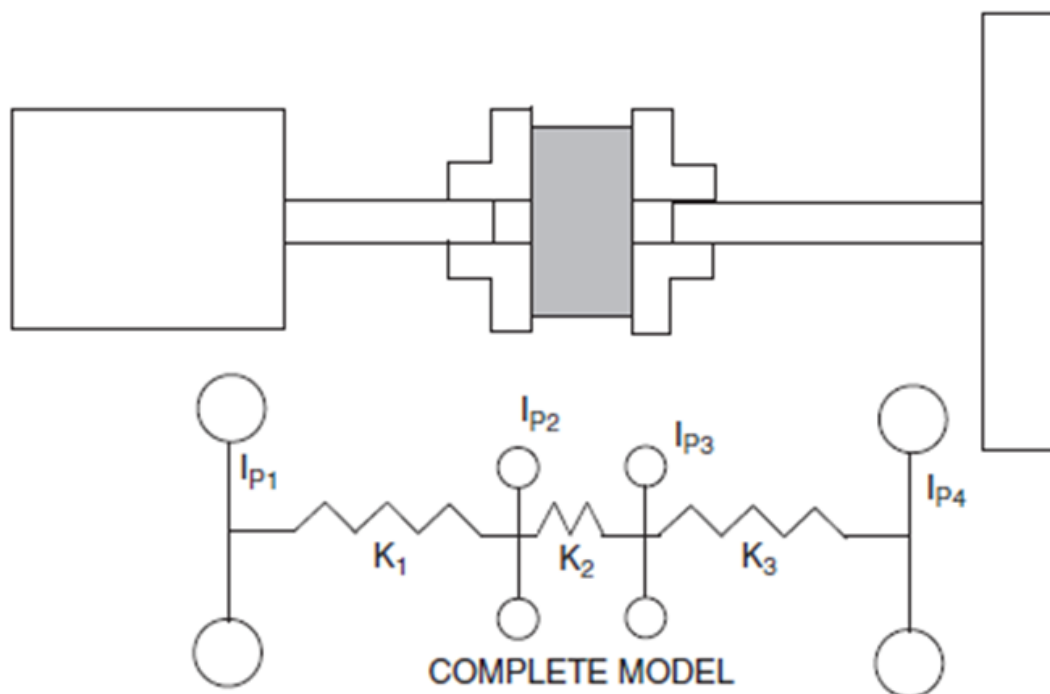


Figure 2.2: Example power system vibration model with simplified stiffness components [19]

Commercial finite element software uses a variety of ROM methods including Arnoldi, Block-Lanczos, and Krylov based computational methods. These methods have historically been the basis for eigenvalue analysis and more recently in ROM [46]. For example, ANSYS-Mechanical uses Mode Superposition Method for reduced order modeling [56], [57], [58].

3. Analytical Model of a Torsional Disk Coupling System

3.1. Assumptions

Mechanical power system designers use analytical models to predict the vibration response of the system. Undesired vibration in a power system can have several negative effects, it can cause: damage to machinery components ultimately affecting lifetime and leading to failure, excessive noise, or even decrease system efficiency [8]. Minimizing resonant frequency vibrations is a factor in preventing catastrophic failure in the system which can lead to long periods of system down time. System failure and down time has a major financial impact in industrial power systems, it is costly for a company in terms of the replacement parts and labor required to become operational again. Thus, engineers use system modeling to prevent such failure.

3.2. Torsional Stiffness

Power system modeling is a combination of spring-mass elements with an added level of complexity. For accurate representation, the engineer must obtain stiffness data from component manufacturers. In this case, we will focus on the shaft coupling component of the system. The shaft coupling itself has an overall stiffness in each degree of freedom it allows for misalignment as well as axially through a parameter called torsional stiffness, sometimes called rotational stiffness. A high torsional stiffness value is desired while allowing for small amounts of inevitable misalignment. Torsional stiffness is the relationship of applied torque and angular deflection. The manufacturer data set may provide the torsional stiffness of the coupling but the methods used to obtain this information can vary throughout the industry and even within a single manufacturer.

An analytical method for finding the stiffness is to break-down the coupling itself and represent the assembly as a combination spring-mass system.

There are several methods of flexible coupling representation and even methods for various modes of misalignment. For example, for angular shaft misalignment there are several modeling methods including: Hooke's joint kinematics and flexible pinned-joint arrangements, [8]. A schematic of the Hooke's joint representation can be seen in Figure 3.1.a. Also, the pinned-joint is a simplified arrangement used by Redmond and depicted in Figure 3.1.b.

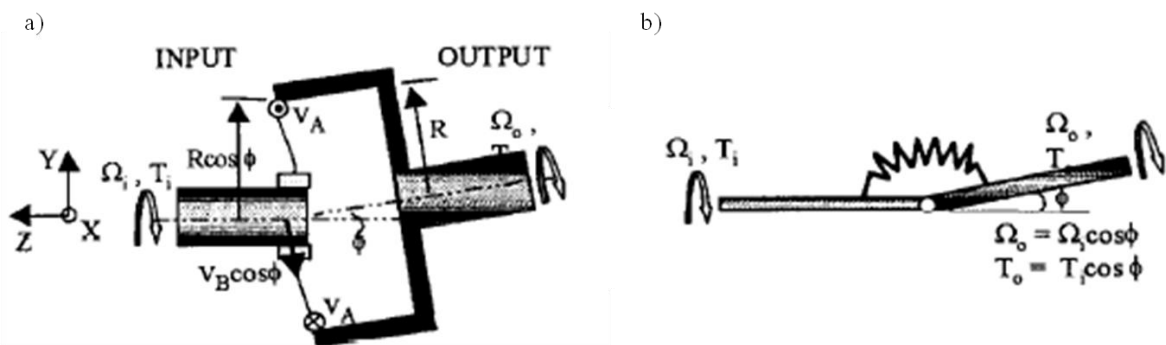


Figure 3.1: a) Hooke's Joint representation b) Pinned-joint representation [8]

Another method to analytically calculate the torsional stiffness of a coupling is to model the axisymmetric geometry cross-sections of each component individually using variations of Eqn. 3.1 then adding them together in series; a method referenced by the American Gear Manufacturers Association (AGMA) 9004 Flexible Couplings standard [59].

$$K_T = \frac{\pi G D^4}{32L} \quad (3.1)$$

where

K_T = torsional stiffness [in-lb/rad]

G = shear modulus, lb/in²
 D = diameter of shaft
 L = length of shaft

A final simplified coupling model may appear as described in Figure 3.2 and Figure 3.3.

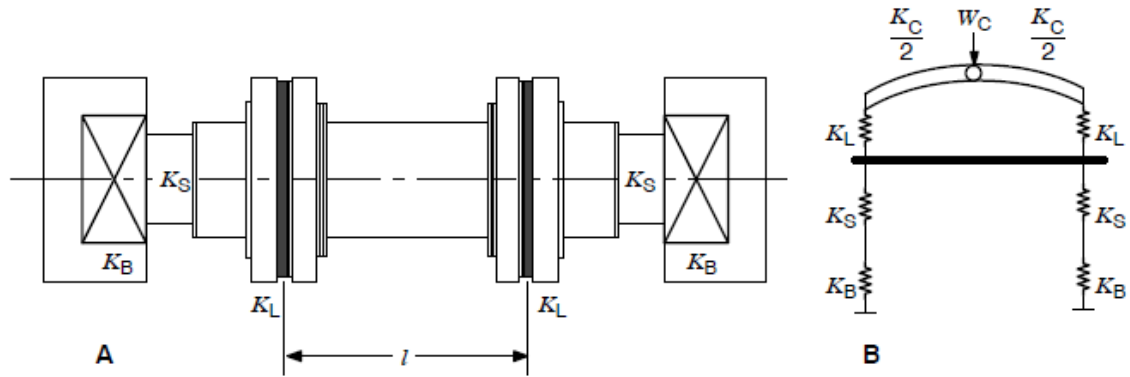


Figure 3.2: Coupling system schematic a) coupling in system b) free-body diagram [59],[10]

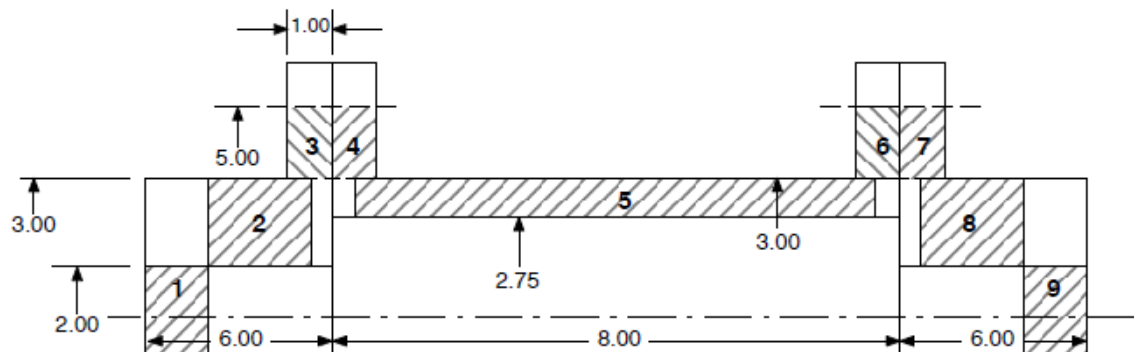


Figure 3.3: Example rigid coupling representation [59]

According to the coupling specification of interest in this study, the theoretical calculations following this method are as follows:

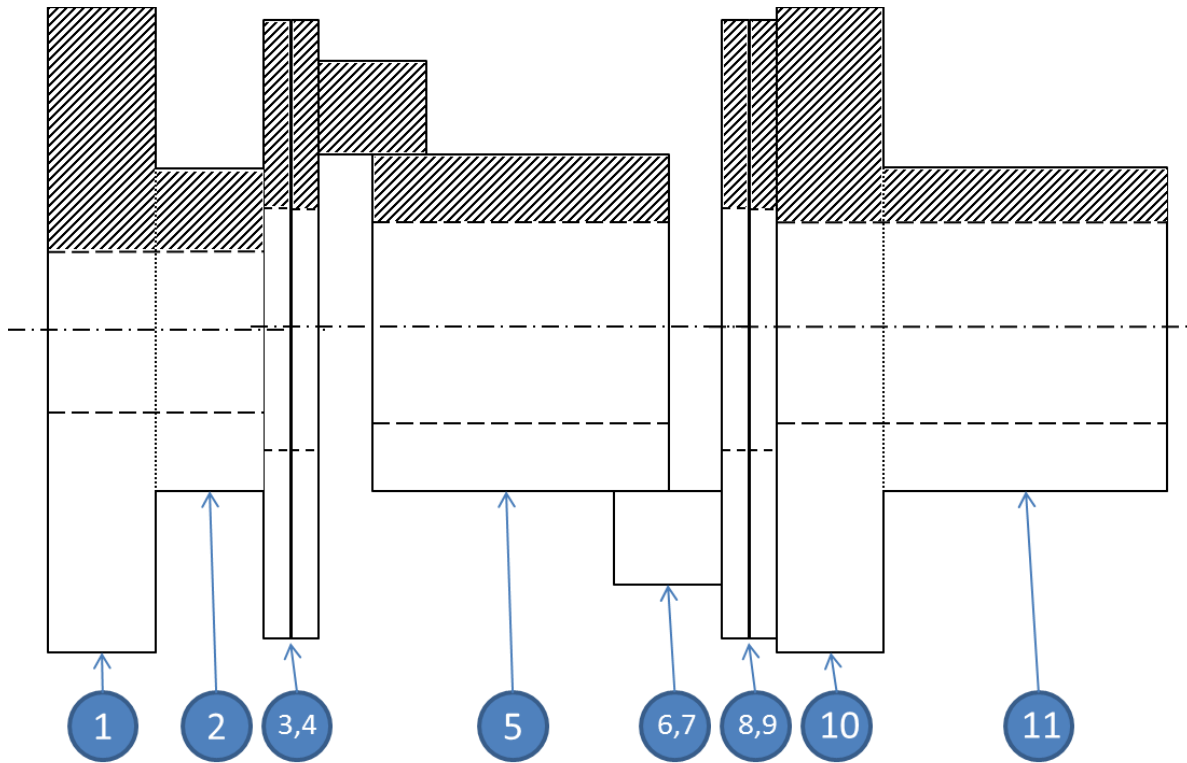


Figure 3.4: Theoretical representation of flexible disc coupling

$$K_T = \left(\frac{1}{K_{End1}} + \frac{1}{K_{CM,f}} + \frac{1}{K_{END2}} \right)^{-1} \quad (3.2)$$

Calculations for Flywheel Adapter

$$K_{1,2,3} = \frac{\pi G}{32L} (D_o^4 - D_i^4) \quad (3.3)$$

$$K_{FA} = \left(\frac{1}{K_1} + \frac{1}{K_2} \right)^{-1} \quad (3.4)$$

$$K_{End1} = \left(\frac{1}{K_1} + \frac{1}{K_2} + \frac{1}{K_3} \right)^{-1} \quad (3.5)$$

Calculations for Center Member

$$K_{4,5,8} = \frac{\pi G}{32L} (D_o^4 - D_i^4) \quad (3.6)$$

$$K_{6,7} = \frac{\pi G D_o^2 D_i^2 t}{(D_o^2 - D_i^2)} \quad (3.7)$$

$$K_{CM,i} = \left(\frac{1}{K_5} + \frac{1}{K_6} + \frac{1}{K_7} \right)^{-1} \quad (3.8)$$

$$K_{CM,f} = \left(\frac{1}{K_4} + \frac{1}{K_{CM,i}} + \frac{1}{K_8} \right)^{-1} \quad (3.9)$$

Calculations for Hub

$$K_{9,10,11} = \frac{\pi G}{32L} (D_o^4 - D_i^4) \quad (3.10)$$

$$K_{Hub} = \left(\frac{1}{K_{10}} + \frac{1}{K_{11}} \right)^{-1} \quad (3.11)$$

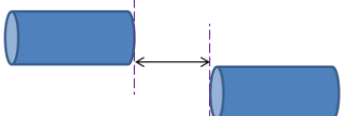
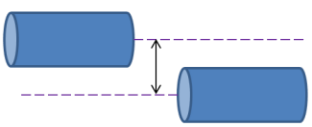
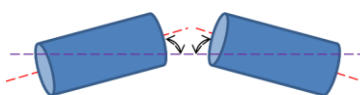
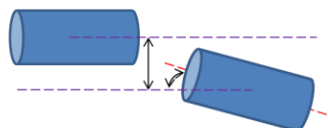
$$K_{End2} = \left(\frac{1}{K_9} + \frac{1}{K_{10}} + \frac{1}{K_{11}} \right)^{-1} \quad (3.12)$$

Implementing these calculations with the values of the coupling in this study yields a torsional stiffness value of: 3.73×10^9 in-lb/rad. The simplified analytical coupling models contain unknowns such as the stiffness influence of bolted connections, flexible element physics, and shaft-hub interface contact.

3.3. Misalignment Stiffness

The implications of forces in the remaining degrees of freedom may be more noticeable during operation. The axial, radial, or angular modes of misalignment induce forces on the rotary system that can produce excessive noise or unwanted vibrations; thus, it is useful to understand the reaction forces they produced. Shaft axial and radial misalignment, are types in which the axis of the connecting shafts experience translational misalignment. Shaft angular offset, in which the axis experience an angular misalignment relative to each other. As well as, a combination of both translational and angular offsets. The German standard DIN 740 Part 2, describes the method of calculating stiffness for each mode of misalignment as shown in the following Table 3.1:

Table 3.1: Overview of shaft misalignment types [60]

Misalignment Type	Schematic	Definition
Shaft Axial		$C_a = \frac{dF_a}{dW_a}$ $F_a = \text{Axial restoring force}$ $W_a = \text{Axial misalignment}$
Shaft Radial		$C_r = \frac{dF_r}{dW_r}$ $F_r = \text{Radial restoring force}$ $W_r = \text{Radial misalignment}$
Shaft Angular		$C_w = \frac{dM_w}{dW_w}$ $M_w = \text{Restoring bending moment}$ $W_w = \text{Angular misalignment}$
Shaft Combination		Combination of Methods

Numerical simulations will represent radial and angular misalignment later in Section 4. The results of the ANSYS simulations will be used to calculate the stiffness of the coupling according to the DIN standard.

4. Full 3-D Numerical Model of a Torsional Disk Coupling System

4.1. Geometry Considerations

The analytical coupling model and experimental results will serve as verification for the 3D numerical model. A parametric approach was used to build the 3D model in a CAD environment (Solidworks) and in the ANSYS environment using the ANSYS Parametric Design Language (APDL) code. This approach is used with the industry professional in mind. With parametric models, different coupling sizes along the spectrum of a product line can quickly be modeled and interpreted; also allowing for the sensitivity analysis of each geometric parameter as well as material and finite element (FE) model parameters as well. Although FE model parameters are included and easily adjusted, this study will provide an accurately tuned ANSYS model for the study of two types of flexible shaft couplings.

First, each coupling component was modeled and assembled in Solidworks according to manufacturer 2D schematics; the 3D model can be seen in Figure 4.1. The 3D models provide a verification and visualization of the component geometry that will be used as reference continuing on to the ANSYS APDL building process.

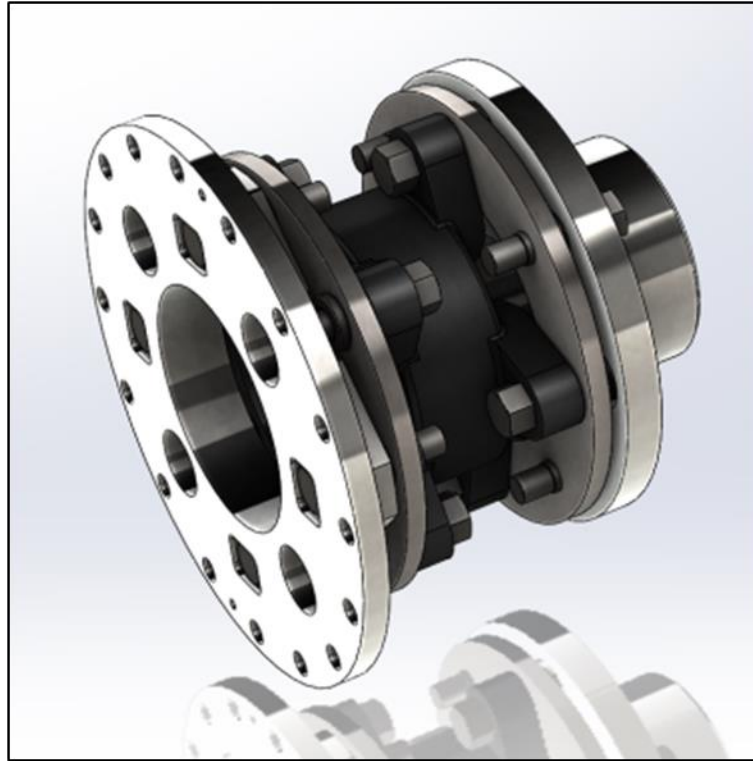


Figure 4.1: 3D Solidworks model of flexible disc coupling

The ANSYS APDL process followed a similar procedure by building each component separately. However, a more robust and automated method was developed for use in ANSYS. An overview of the user experience is simple: the user is able to input all parameters in a text file and then run an APDL script that will read the desired parameters, build all components, import the components into a separate ANSYS model, prepare the assembly and solve the model; see Figure 4.2. The automated ANSYS script allows for less experienced users to set-up and solve a complicated ANSYS model while also allowing more experienced users to investigate more detailed adjustments of the model and ultimately a product in their product line.

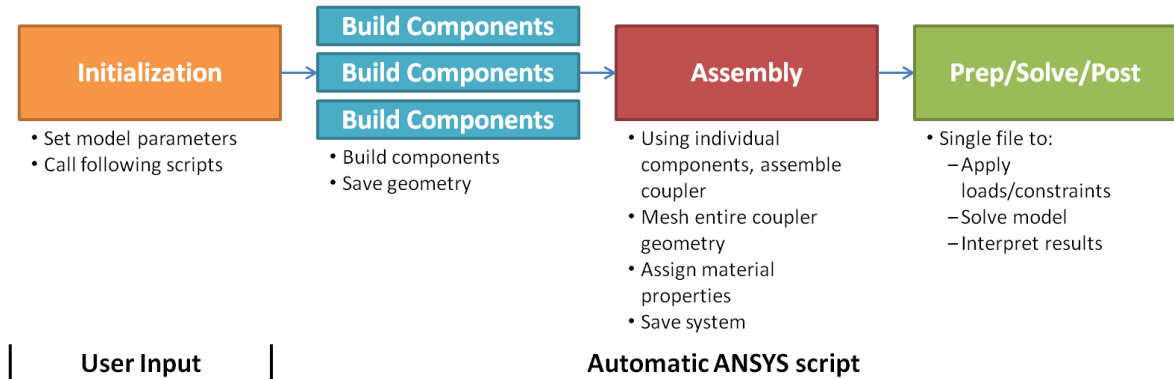


Figure 4.2: ANSYS Automatic script procedure

Although the model creation and parameterization is more robust and automated with the APDL script, the actual geometry was simplified. Geometry simplification is a common technique in finite element modeling (FEM) to generate an appropriate mesh of the components while maintaining a reasonable solution time. In order to simplify the geometry, the de-featuring removed small rounds and chamfers which do not have a critical impact on mode shapes or overall coupling stiffness. However, it must be noted that these features play an important role in actual use for appropriate stress distribution in the part. The absence of the features affects the study of coupling component strength analysis.

4.2. Material Selection and Assumptions

The material properties of each component were chosen based on manufacturer specifications [2]; see Table 4.1 [61], [62], [63], [64], [65]. An assumption was taken to consider material properties as linear rather than non-linear in consideration of solution time for the large full coupling assembly model of this study. Since there is a diverse range of flexible disk couplings and manufactures in the marketplace, variation of material selection is inevitable. For example, a manufacturer may recommend a specific

SAE or ASME bolt grade to be used with their coupling while the customer may choose bolts that are readily available and do not follow the recommendation. Thus, a study of the impact that each material property has on torsion stiffness was conducted. The resulting changes in material properties are compared in Figure 4.3 and summarized in Table 4.2. The material properties of the hub and center member components have the largest impact on coupling torsional stiffness.

Table 4.1: Component Material Properties

Component	Material	E (psi)
Hub	4140 Steel	2.97E+07
Discs	4140 Steel	2.97E+07
Center Member	Cast Steel	2.83E+07
Flywheel	Cast Iron	1.80E+07
Adapter Bolts/ Washers	4140 Steel	2.97E+07

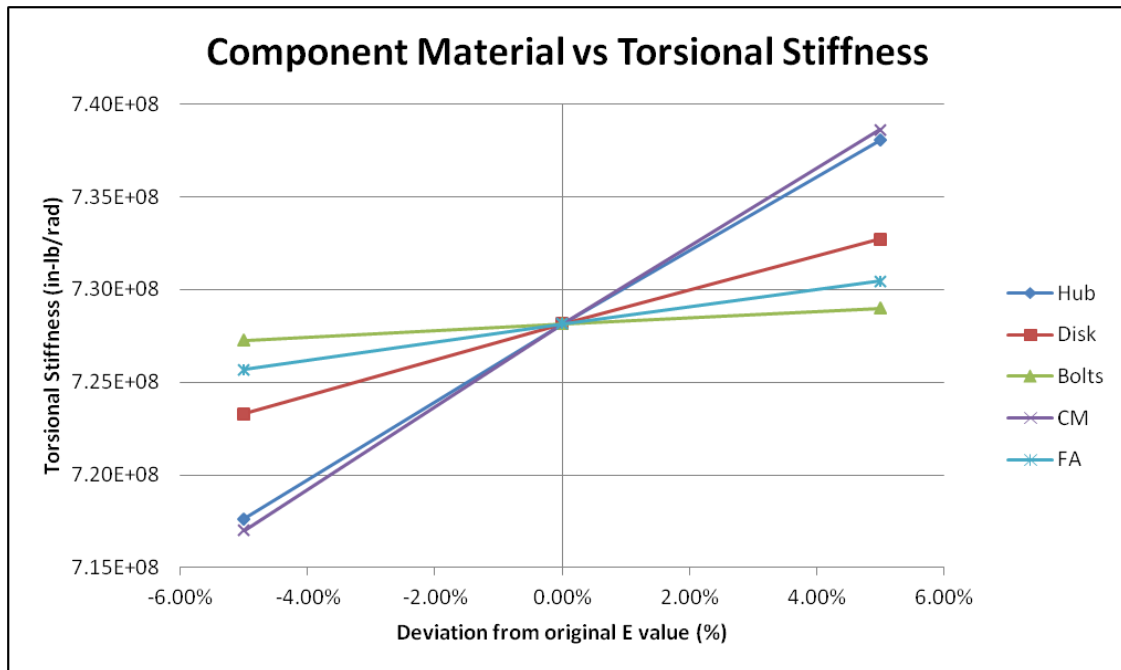


Figure 4.3: Diagram comparing the change in material properties of each component

Table 4.2: Material property study results Summary

Component	Material	ΔE_{Mat}	K_T	$\Delta K_{T, val}$	$\Delta K_{T, \%}$
Hub	4140 Steel	+5%	7.38E+08	-9.89E+06	-1.36
Hub	4140 Steel	-5%	7.18E+08	1.05E+07	1.45
Disk	4140 Steel	+5%	7.33E+08	-4.57E+06	-0.63
Disk	4140 Steel	-5%	7.23E+08	4.88E+06	0.67
Bolts	4140 Steel	+5%	7.29E+08	-8.44E+05	-0.12
Bolts	4140 Steel	-5%	7.27E+08	8.95E+05	0.12
Center Member	Cast Steel	+5%	7.39E+08	-1.05E+07	-1.44
Center Member	Cast Steel	-5%	7.17E+08	1.12E+07	1.53
Flywheel Adapter	Cast Iron	+5%	7.30E+08	-2.28E+06	-0.31
Flywheel Adapter	Cast Iron	-5%	7.26E+08	2.49E+06	0.34

4.3. Modeling Flexible Disk Pack - Contact Analysis

A similar metric to the adjustment of component parameters that affects the overall torsional stiffness of a coupling is the number of disc used in the combined disc pack. The parameters of disc pack component and to what effect these parameters have on the overall torsional stiffness is necessary to understand. The disc shape, thickness, and quantity can vary across manufacturers but are all relevant as the flexible element of the coupling [10], [9], [35]. These components account for shaft misalignment and transmit torque through the system. For simplification, the disc pack was initially modeled as a single solid component. The parametric thickness of the solid is studied to interpret the effect on overall coupling torsional stiffness. The specific coupling used in this study has a standard disc pack size of approximately 40 individual discs. The thickness study conducted investigates disc pack sizes of 20, 30, 40, and 50 discs. The results of the study conclude that the disc pack thickness indeed affects the overall torsional stiffness of the coupling which is anticipated as the disc pack is the flexible element of the assembly, Figure 4.4 along with Table 4.3 display the results.

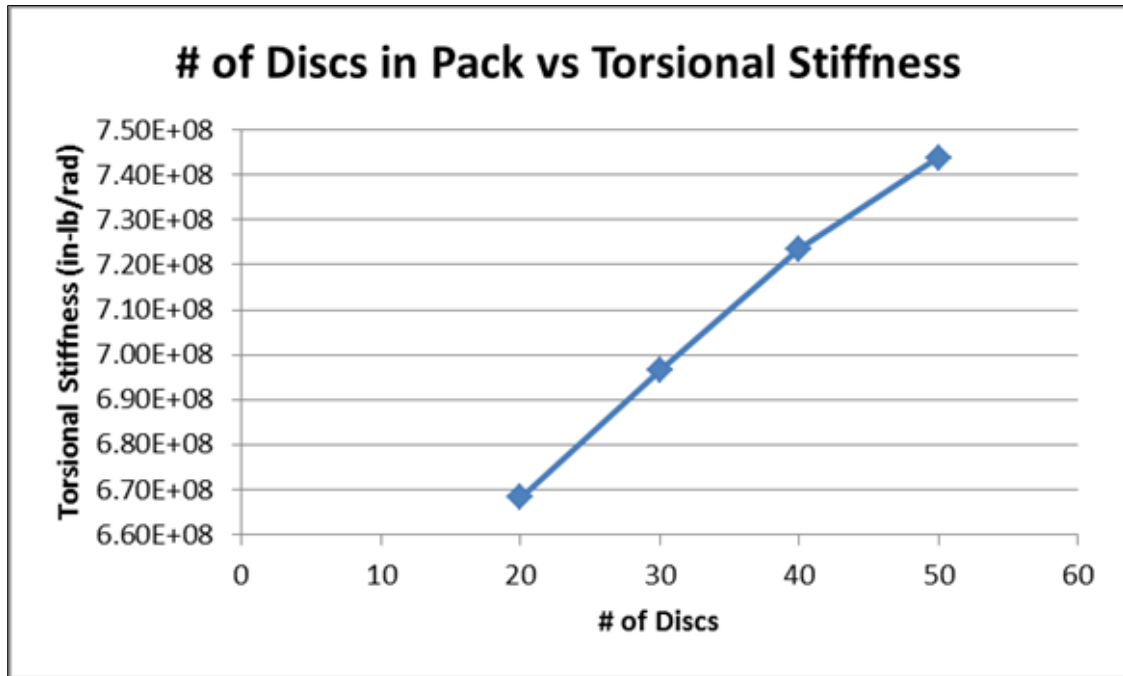


Figure 4.4: Influence of disc pack thickness on K_T

Table 4.3: Disc pack thickness data and deviation from the original value

Disk #	K_T (in-lb/rad)	Δ , val
20	6.68E+08	5.99E+07
30	6.96E+08	3.17E+07
40	7.23E+08	4.70E+06
50	7.44E+08	-1.56E+07

However, the disc pack contains multiple individual discs which are too thin to model in detail as components in the entire coupling assembly. In such case, an investigation of effective disc properties was conducted. In reality the disc pack contains multiple disks and as such a numerical approach using FEA was conducted using contact elements between each disc layer. The analysis was constructed as a simplified representation of the full disc pack. A section of the pack between bolt locations was

isolated and modeled as a stack of thin rectangular plates with a length equal to that of the arc length between bolt locations; Figure 4.5. The ANSYS FE model, represented by Figure 4.6, was constrained at one end with a 1 in-lb moment applied to the other. For initial to verification of the method, a small moment and only three discs were used since the full disc pack is computationally expensive with non-linear contact elements between each disc pair.

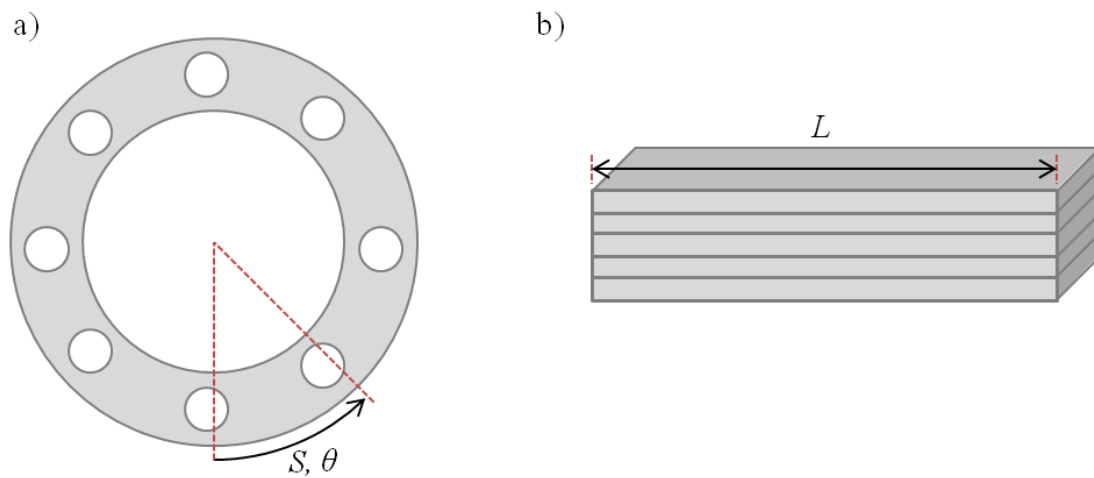


Figure 4.5: a) isolated disc pack section (top view) b) disc pack model (side view)

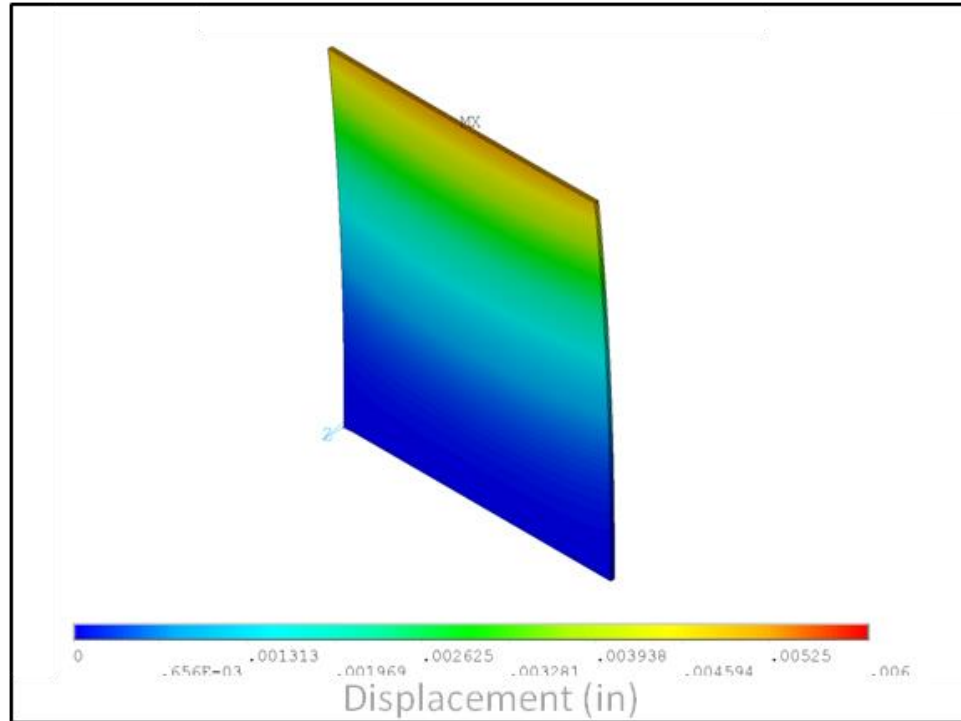


Figure 4.6: ANSYS disc pack model deformed state (3-disc layers)

In theory, since the disc pack is a stack of isotropic material the effective solid can be interpreted as transverse isotropic. Material properties in the X-,Y-, and Z- material directions are the same in tension and compression as the isotropic material, but there exists an alternative shear modulus from the presence of multiple disc layers. The FEA results were used to characterize the effective material properties of the bulk component. The characterization followed an even further simplification of the model using Timoshenko Beam Theory. Accounting for shear, the Timoshenko Beam Theory is a simple FE approach to this problem [66], [67]. The geometry can be modeled as a two-node, single beam system with the same constraints and loads as in the FE model; such that represented by Figure 4.7.

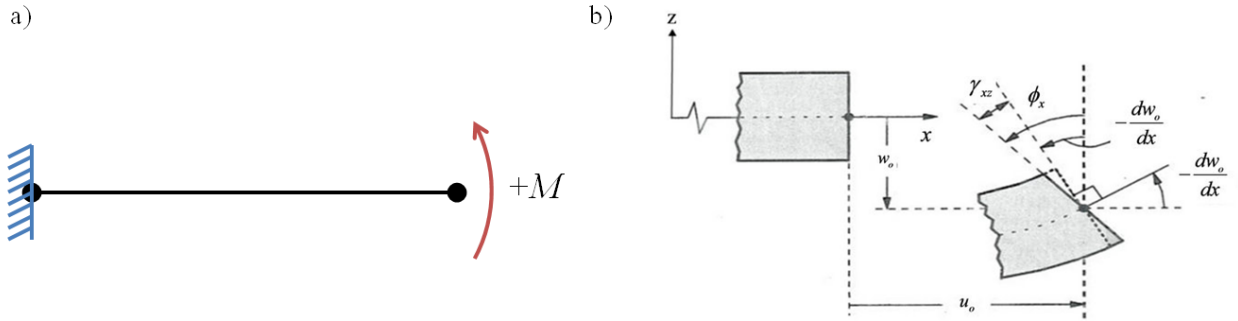


Figure 4.7: : a) Beam constraints b) Timoshenko standard beam model [67]

The goal of the following theoretical procedure is used to extract the shear modulus using Timoshenko Beam Theory.

First, the Global Stiffness Equation, Eqn. 4.1, is the basis of finite element modeling.

$$[K]\{d\} = \{F\} \quad (4.1)$$

The stiffness matrix corresponding to the Timoshenko Beam theory is as follows in Eqn. 4.2:

$$[K] = \frac{EI}{L^3(1+\hat{\varphi})} \begin{bmatrix} 12 & 6L & -12 & 6L \\ 6L & (4+\hat{\varphi})L^2 & -6L & (2-\hat{\varphi})L^2 \\ -12 & -6L & 12 & -6L \\ 6L & (2-\hat{\varphi})L^2 & -6L & (4+\hat{\varphi})L^2 \end{bmatrix} \quad (4.2)$$

$$\text{where } \hat{\varphi} = \frac{12EI}{(kAGL^2)}$$

and k_s = shear coefficient, A = characteristic area, G = shear modulus, L = characteristic length

The current study utilizes the 2-node single beam model as shown in Figure 4.7-a of which the Beam equation is represented in Eqn. 4.3.

$$[K] \begin{Bmatrix} d_1 \\ \varphi_1 \\ d_2 \\ \varphi_2 \end{Bmatrix} = \begin{Bmatrix} F_1 \\ M_1 \\ F_2 \\ M_2 \end{Bmatrix} \quad (4.3)$$

After taking into account the corresponding constraints and loading of the 2-node beam, Eqn. 4.3 can be simplified into Eqn. 4.4.

$$\begin{bmatrix} 12 & -6L \\ -6L & (4 + \hat{\varphi})L^2 \end{bmatrix} \begin{Bmatrix} d_2 \\ \varphi_2 \end{Bmatrix} = \begin{Bmatrix} F_2 \\ M_2 \end{Bmatrix} \quad (4.4)$$

Another representation of Eqn. #4-4 is the system of two beam equations shown in Eqn. 4.5 and Eqn. 4.6:

$$\frac{EI}{L^3(1+\hat{\varphi})} [(12)d_2 + (-6L)\varphi_2] = F_2 \quad (4.5)$$

$$\frac{EI}{L^3(1+\hat{\varphi})} [(-6L)d_2 + (4 + \hat{\varphi})L^2\varphi_2] = M_2 \quad (4.6)$$

This system of equations can best use Eqn. 4.6 for the extraction of the modulus value. After substituting in the values for $\hat{\varphi}$, the resulting shear modulus, G , can be solved for and represented as follows with Eqn. 4.7.

$$G = \frac{12EI\left(\varphi_2 - \frac{M_2L}{EI}\right)}{k_s A \left(\frac{M_2L^3}{EI} + 6Ld_2 - 4L^2\varphi_2\right)} \quad (4.7)$$

Now, with the derivation of shear modulus for the system, the bulk shear modulus value can be calculated based on the available results. For verification purposes, the disc pack simulation containing multiple discs was compared to a solid disc pack simulation;

see Figure 4.8. The resulting shear modulus values, G , for the disc pack studies are shown in Table 4.4.

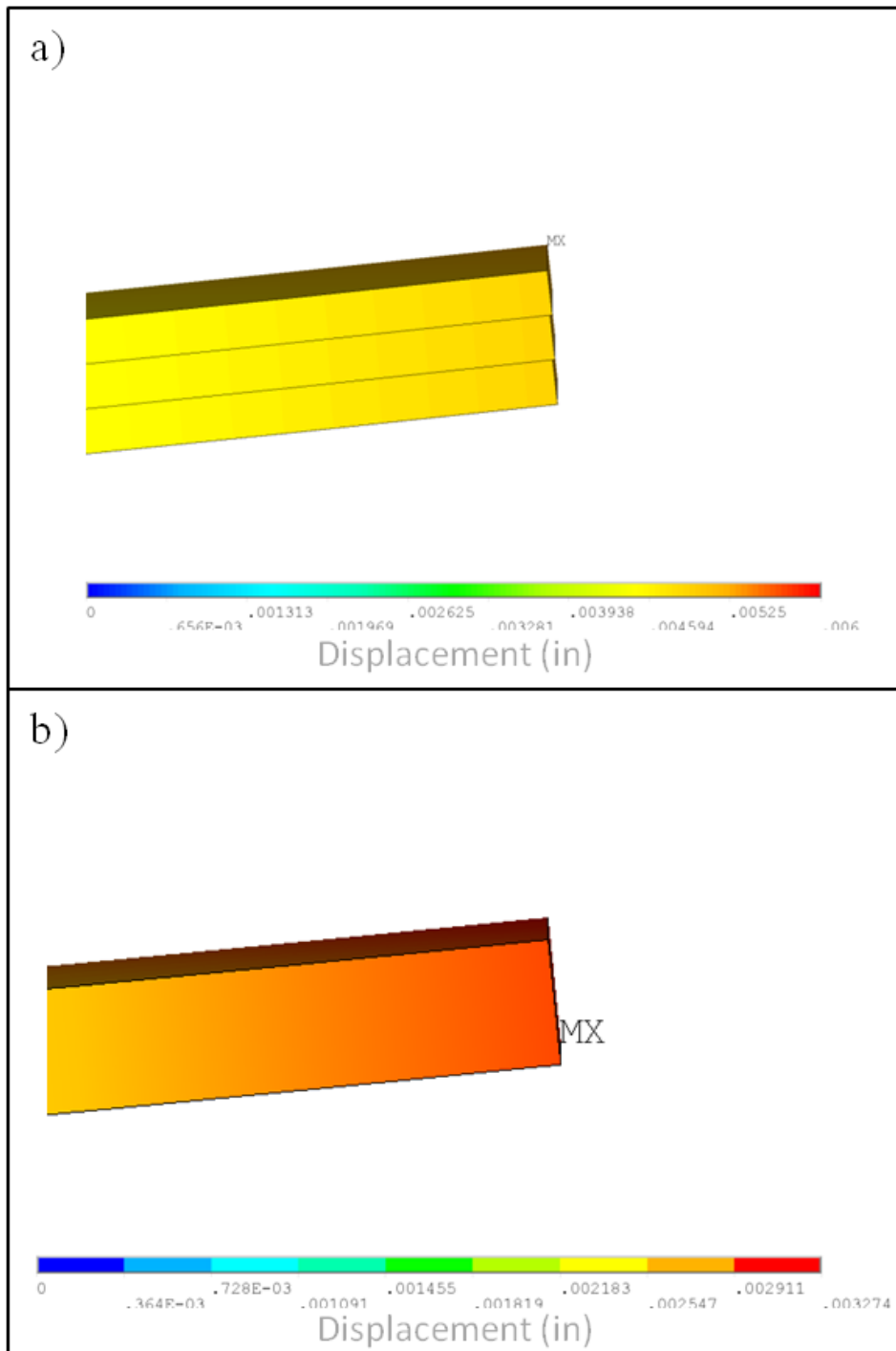


Figure 4.8: Disc pack FE model comparison a) multiple discs b) solid disc pack

Table 4.4: Shear modulus comparison

Method	G (lb/in ²)	$\Delta\%$,theory
Theoretical	1.159E+07	
Multi-Disc	3.995E+08	33.48
Single-Disc	3.995E+08	33.48

The simulation results comparing the multiple layer disc pack and single homogenous disc pack generate a shear modulus of no significant difference from each other with a difference below 1%. However, the comparison of these results to the accepted shear modulus of steel yields a 33% difference; indeed there is room for improvement and further investigation of this method.

4.4. Eigenvalue Analysis - Natural Modes of Vibration

The parameters studied and their effect on torsional stiffness is discussed; of greater importance is the effect of torsional stiffness and misalignment on vibration in a power system. Unwanted vibrations can cause unexpected failure of the system and can harm more expensive drive equipment in connection with the coupling system [68], [69], [70]. This study is of the natural frequencies of the simplified coupling geometry; limited by the computational resources, the disc pack was modeled as an effective solid component rather than a stack containing multiple discs. The study was conducted in the ANSYS environment which uses the Block-Lanczos method to solve for modal analysis [56]. The first 20 modes were solved and analyzed from the ANSYS results. The mode shape results are classified and summarized in Table 4.5.

Table 4.5: Summary of Mode Shapes and Results

Mode (#)	Frequency (Hz)	Type
1	0.00	rigid
2	0.00	rigid
3	0.00	rigid
4	0.00	rigid
5	0.00	rigid
6	0.00	rigid
7	10.70	lateral bending
8	10.70	lateral bending
9	12.21	lateral tension
10	18.11	CM Wobble
11	18.11	CM Wobble
12	19.29	Disk(FA) Flexure
		CM lateral displace
13	22.48	
14	24.68	FA flexure
15	25.70	Torsional
16	37.66	CM/FA Flexure
17	38.31	FA Flexure
18	38.31	FA Flexure
19	38.70	CM Flexure
20	41.57	FA Flexure

The first six modes correspond to the unconstrained six degrees of freedom for the solid body while the rest contain modes of lateral bending, tension, axial torsion, and component flexure or wobble. The classification of later vibration modes includes the uni-axial bending of the entire system and tension from each end of the system; Figure 4.9. Also, the component modes include those of center member wobble and translation corresponding to modes 11 and 13 respectively and depicted by Figure 4.10. Additional component flexure includes that of the disc and flywheel adapter for modes 12 and 14 respectively shown in Figure 4.11. Finally, torsional vibrations are important to be aware of in terms of the lifetime of the coupling; corresponding to mode 15 of this study, Figure 4.12 displays one torsional natural frequency.

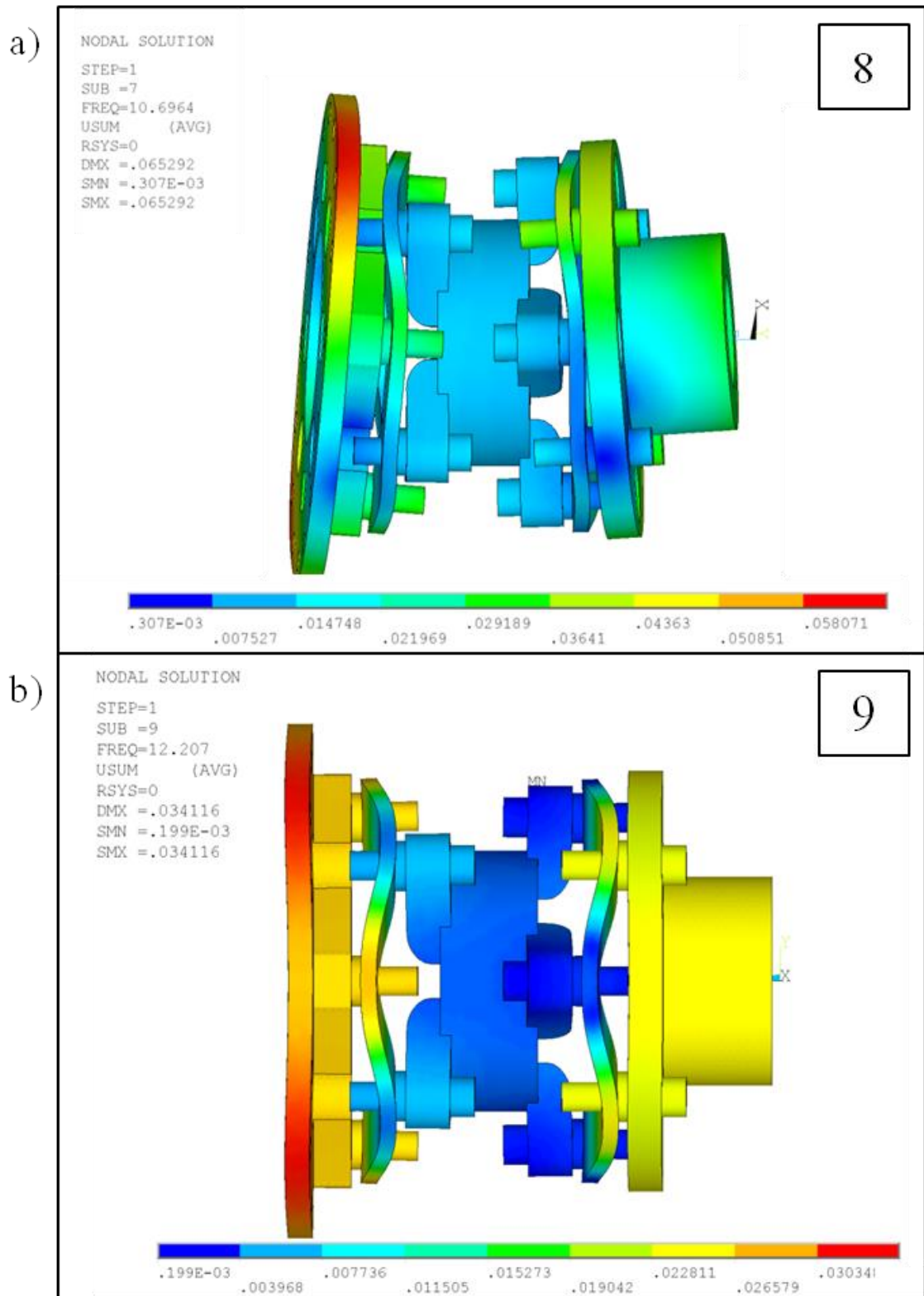


Figure 4.9: Lateral Modes: a) Mode 8 - Bending and b) Mode 9 – Tension

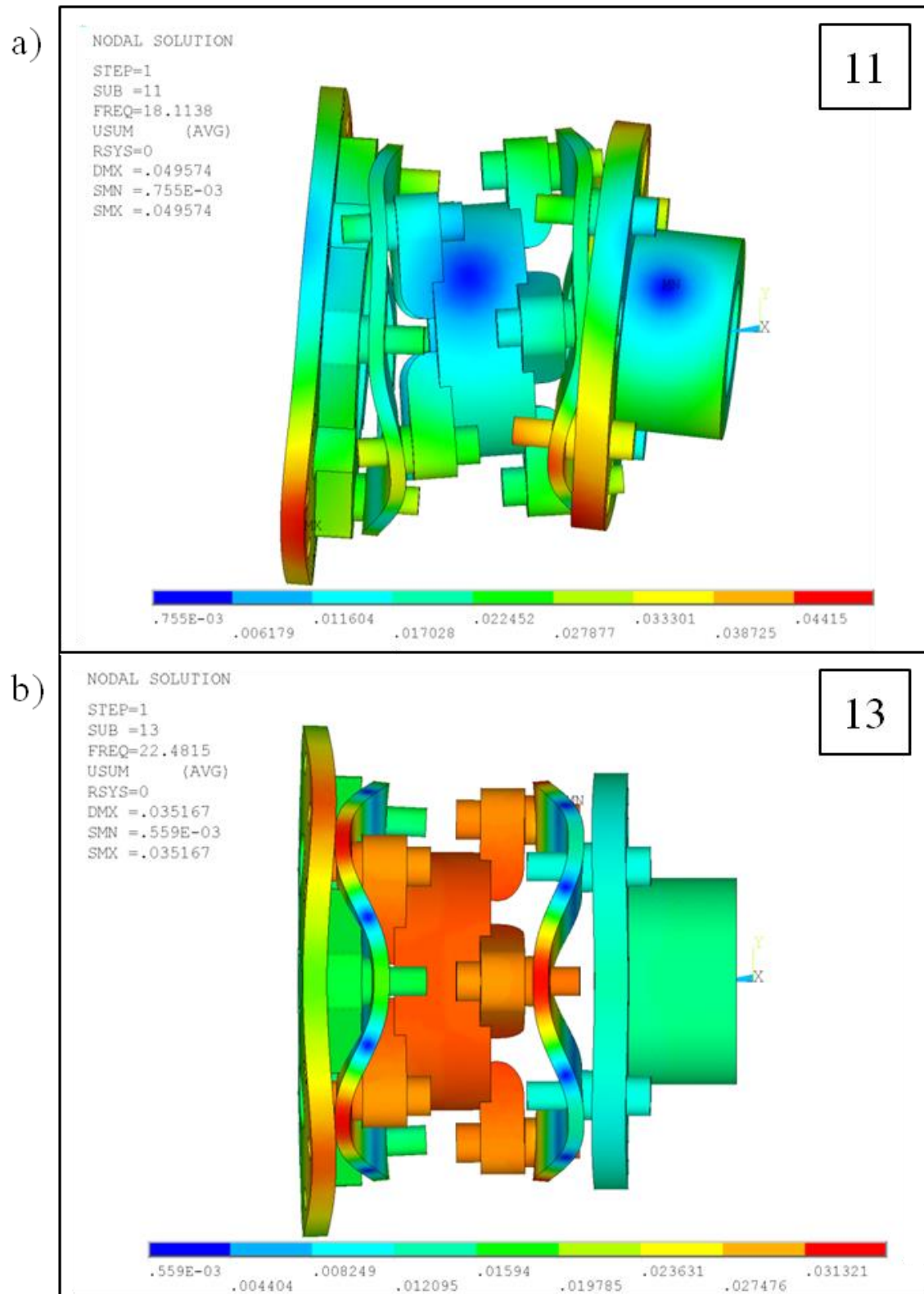


Figure 4.10: Center Member mode shapes: a) Mode 11 - Wobble and b) Mode 13 – Translation

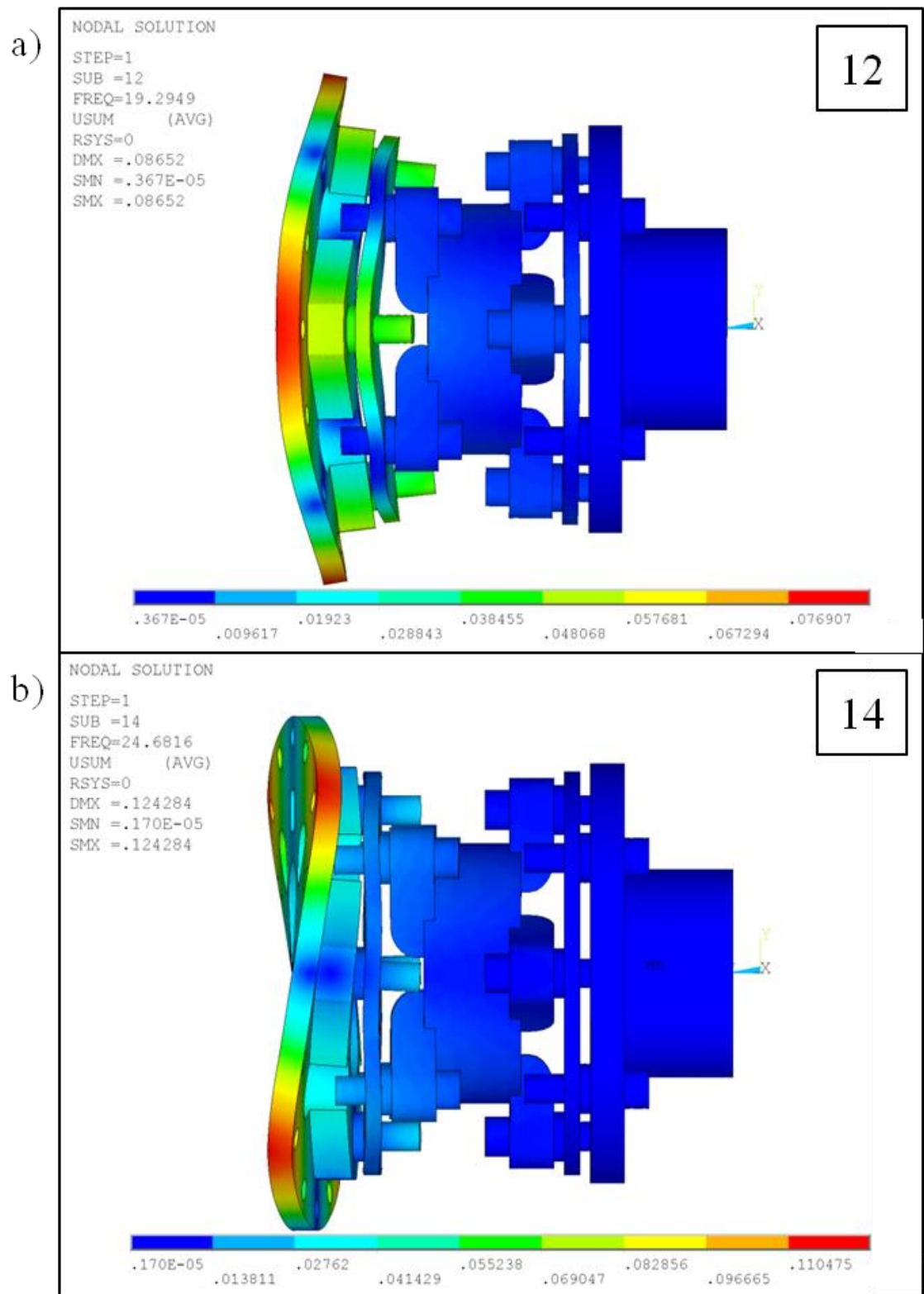


Figure 4.11: a) Mode 12 – Disc Flexure and b) Mode 14 – Flywheel Adapter Flexure

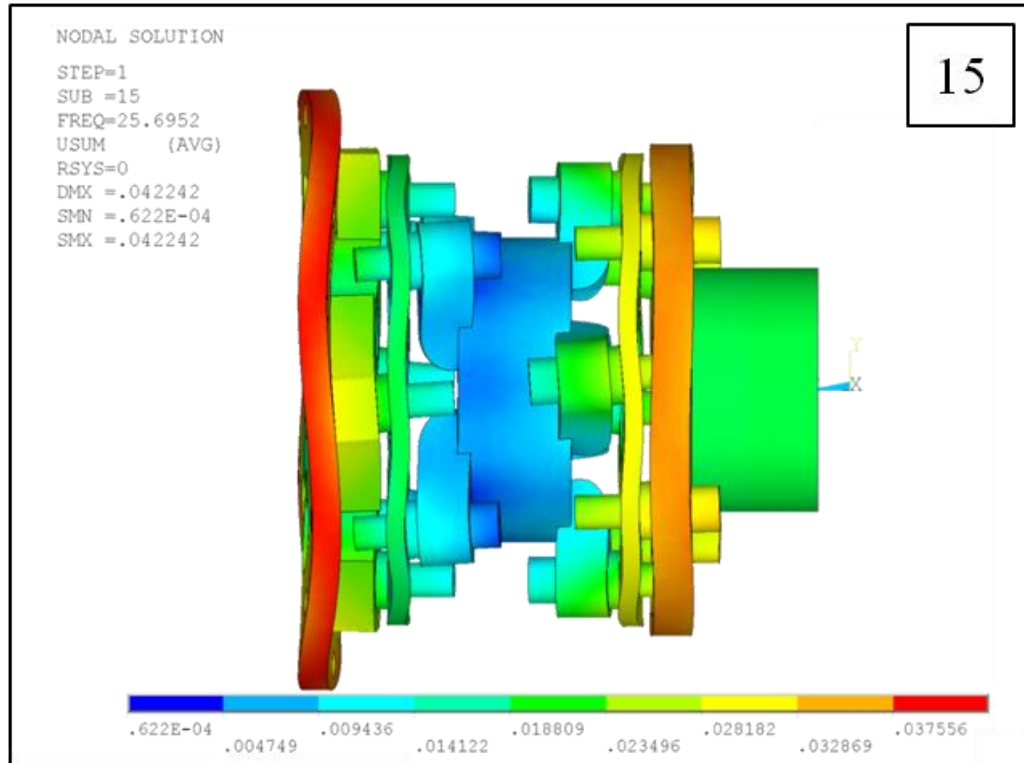


Figure 4.12: Mode 15 – Torsional Frequency

4.5. Steady State Static Analysis - Torsional and Bending Stiffness

In this study ANSYS has been verified as a useful tool for analyzing the mode shapes of the flexible coupling. The results can be analyzed to determine natural frequencies of the assembly and these natural frequencies can be accounted for when analyzing the entire power system. The vibration results reveal modes of potential misalignment and torsional harmonics of which the stiffness properties are critical influences of the result. As such, the static torsional stiffness properties can be analyzed through an independent study and the modal analysis can be leveraged in using reduced order modeling techniques.

In comparison to the analytical method for determining torsional coupling stiffness from Section 3.2, the ANSYS numerical method utilizes the more robust 3D geometry developed for the previous simulation studies of material properties, disc thickness, and modal analysis. The simulation model was prepared for an axial torque application through the corresponding hub with the opposite end constrained and there are two methods which will be used to do so.

The first method accounts for a rigidly constrained end and input shaft which would directly correspond to how an actual coupling is constrained in real practice or experimentation; see Figure 4.13. These rigid ends are modeled and meshed with the entire coupling assembly. The input shaft extends outward from the hub component where the torque is applied to the outside nodes. The fixed end is modeled as rigidly constrained bolts which are connected through the bolt holes of the flywheel adapter.

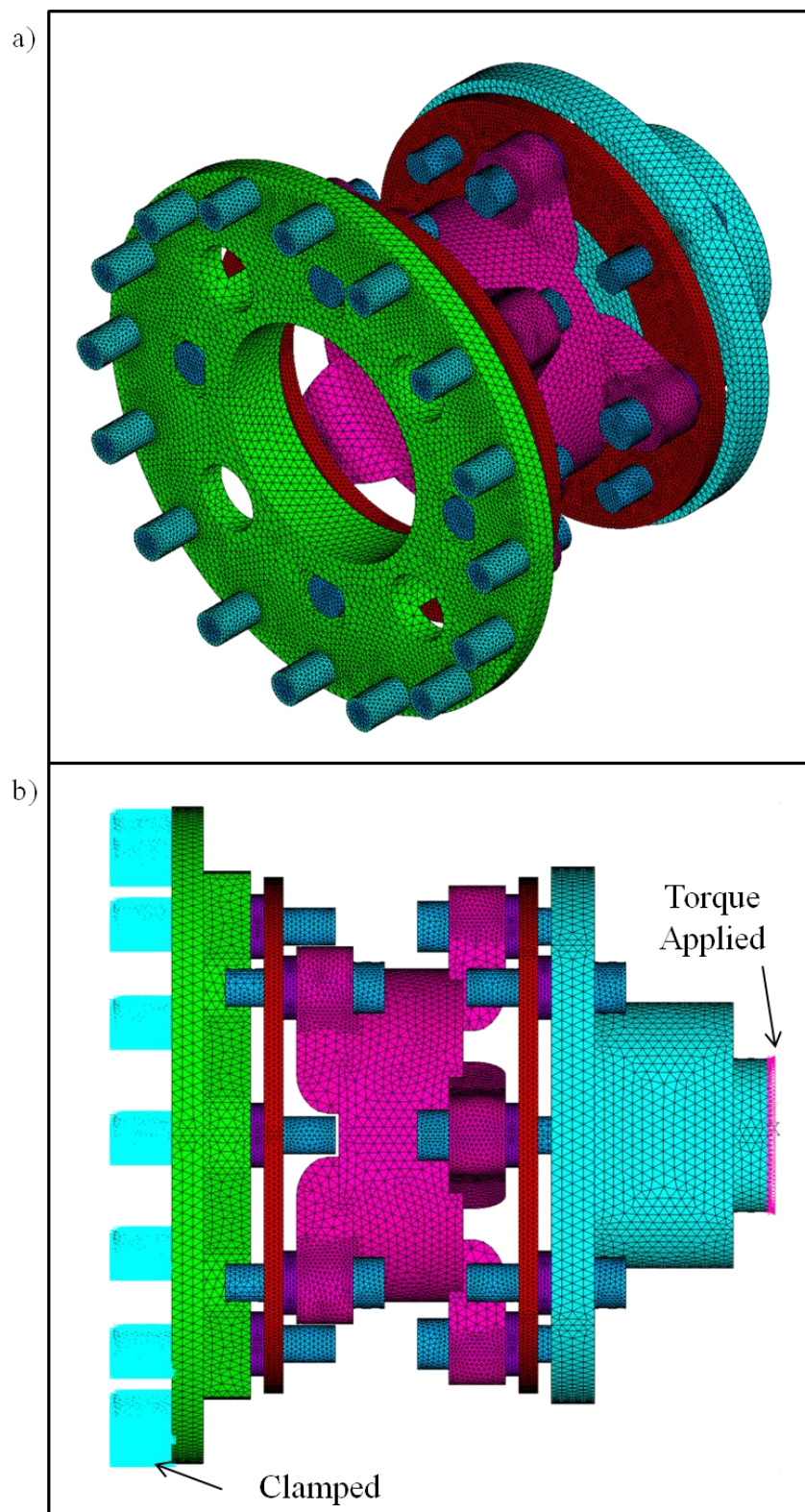


Figure 4.13: a) Method 1 geometry b) Method 1 loads and constraints

The second method is specific coupling assembly with loads and constraints applied directly; see Figure 4.14. Again, the interior nodes of all bolt holes of the flywheel adapter which would secure the coupling to another system component are constrained. The torque load is applied to the interior nodes of the opposite end inside the hub bore and according to the ANSI/AGMA 9004 shaft 1/3 rule [59]. The shaft 1/3 rule states that the input torque is transmitted by the input shaft for 1/3 the connecting hub bore then the remaining torque is transmitted through the hub itself.

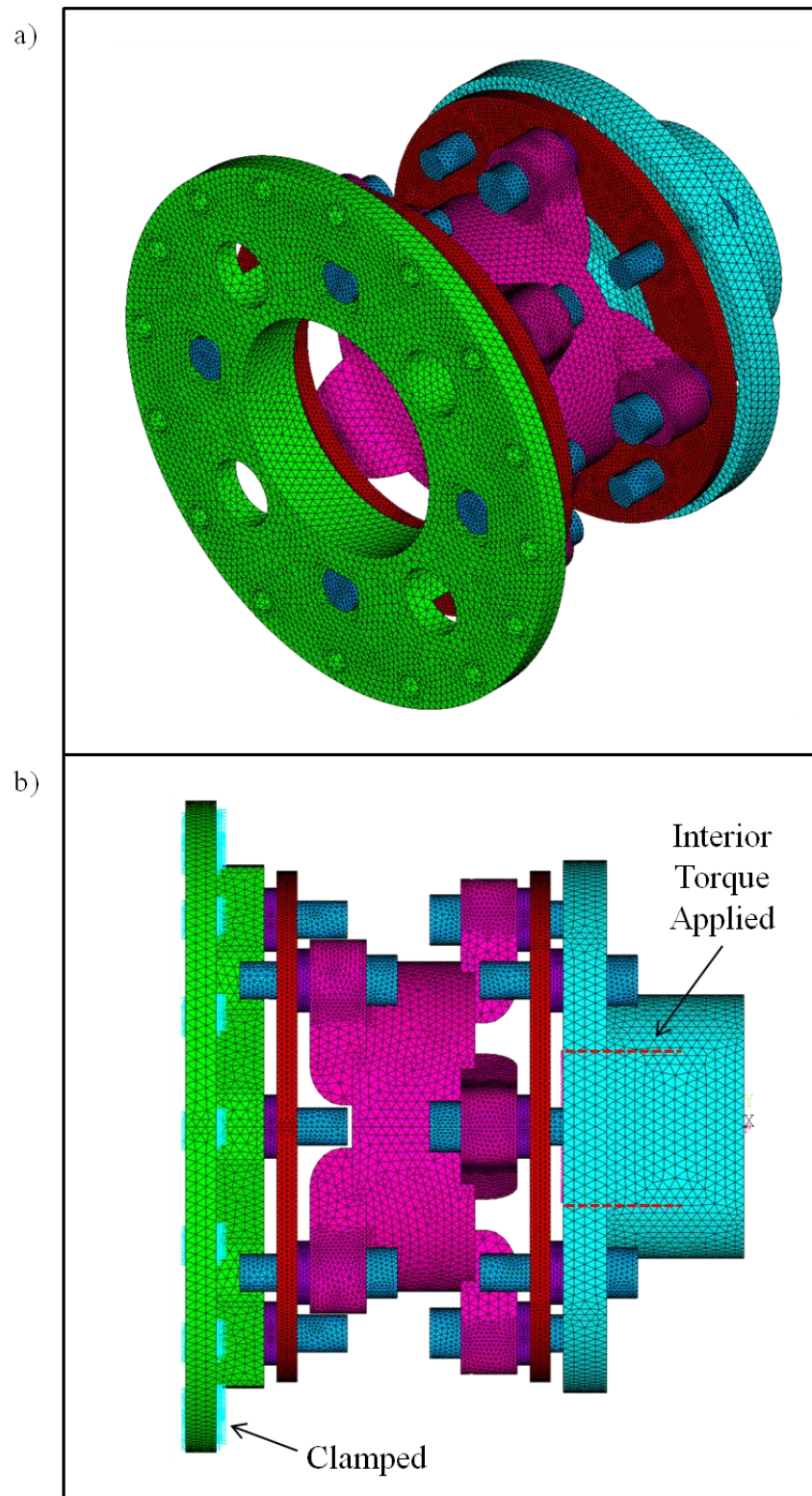


Figure 4.14: a) Method 2 geometry b) Method 2 loads and constraints

In comparison, the two methods have benefits and disadvantages. The first method that accounts for rigid ends is identical to loading in practice, but does not match theoretical calculations accounting for the shaft 1/3 rule and is influenced by the number of rigid bolts securing the flywheel adapter. The second method is beneficial by isolating the coupling itself eliminating additional contributions to the overall torsional stiffness of the assembly and accounting for the theoretical shaft 1/3 rule.

The coupling in question is rather large with a hub internal bore over 8 inches in diameter and is designed for high-torque/low-speed applications. The torque was applied to the hub component with a value of 1.5 M-in-lb, a value near the maximum recommended torque from the manufacturer. ANSYS solution options were set to a static linear analysis with 10 incremental load steps leading to the final applied torque value. During post processing of the results a script was created to interpret the angular displacement and reaction forces at the location of applied torque. These results are plotted in Figure 4.15 as Torque vs. displacement angle illustrating torsional stiffness as the slope of the line. In this case, the relationship between each point is linear when in practice the actual torsional stiffness is a non-linear relationship affected by non-linear material properties, fatigue, and hysteresis. Final torsional stiffness values from simulations using Method 1 and Method 2 are depicted in Table 4.6.

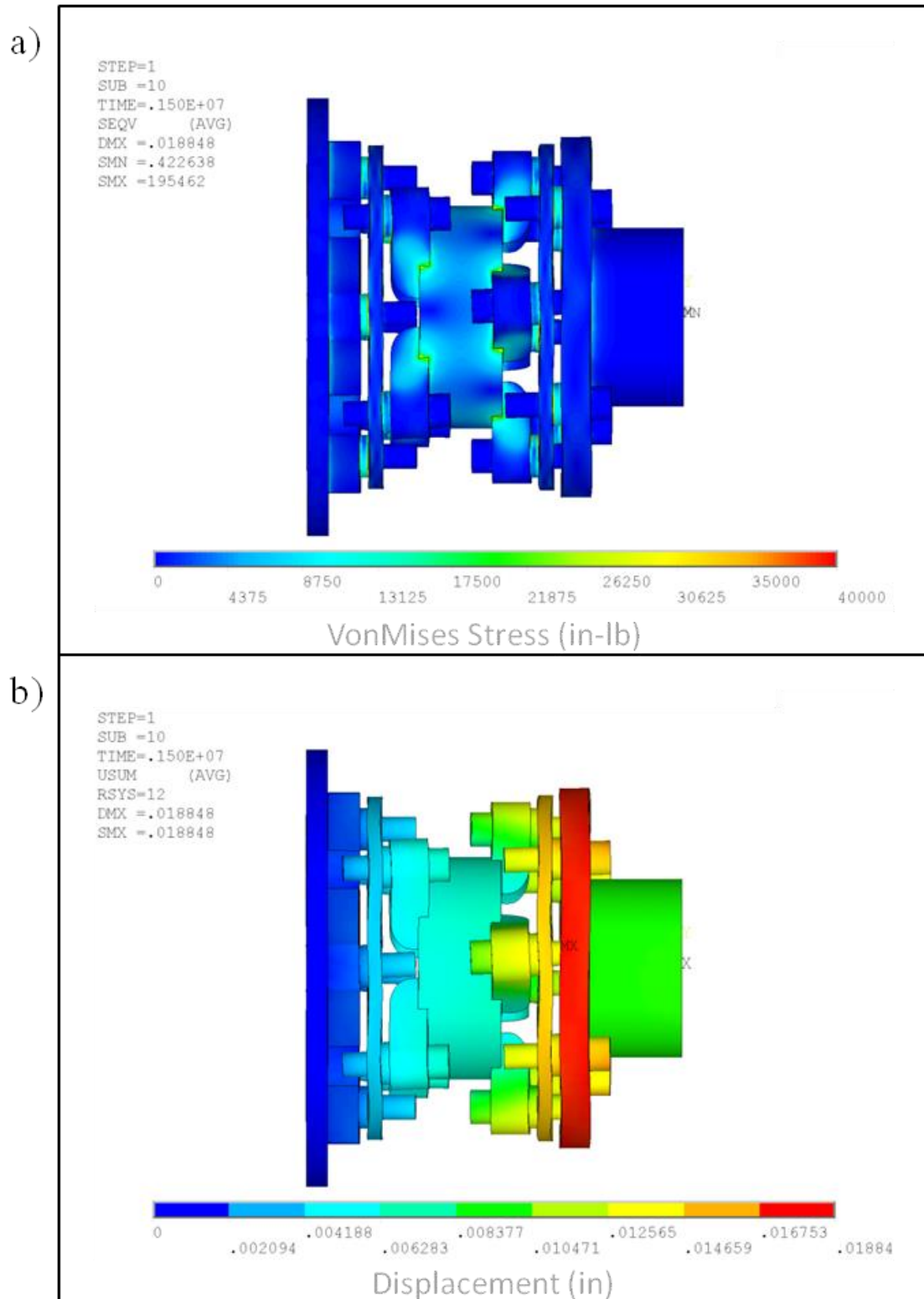


Figure 4.15: ANSYS Method 1 simulation result a) Von Mises stress b) Displacement sum

Table 4.6: Method vs Torsional Stiffness

Method	K_T (in-lb/rad)	$\Delta, \%$
1	7.28×10^8	+46.98%
2	10.7×10^8	

The theoretical calculation of torsional stiffness often varies by manufacturer. In this study, the theoretical method of calculating torsional stiffness referenced by ANSI/AGMA 9004 is used with results compared to an identical ANSYS representation. The ANSYS representation depicted in Figure Figure 4.16 is compared with the theoretical results from Section 3 in Table 4.7.

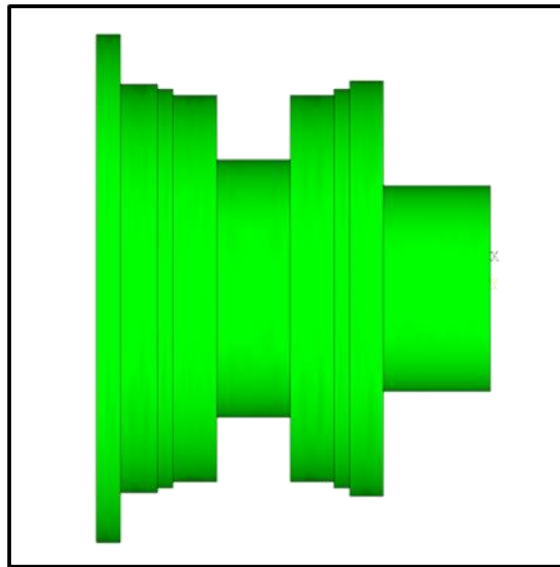
**Figure 4.16: Simplified ANSYS representation**

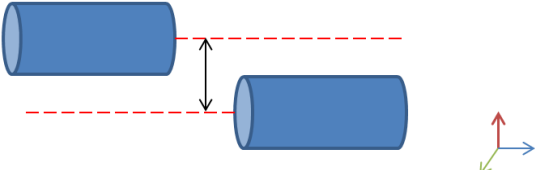
Table 4.7: Theoretical torsional stiffness result accuracy

Parameter	Value	Units	Δ
$K_{T,theory}$	3.73×10^9	in-lbs/rad	38%
$K_{T,ANSYS}$	2.33×10^9	in-lbs/rad	

In addition to torsional stiffness, the stiffness in other degrees of freedom is also important when considering for misalignment. A study of misalignment stiffness was conducted on the geometry used previously in Method 2; with this geometry, a misalignment can be applied directly to the coupling without the need for rigid input shafts or constraining bolts that may influence the results.

A specific study in ANSYS was conducted for axial shaft misalignment stiffness. Similar to the torsional stiffness studies, a force was applied at the driving hub component, but in the Cartesian y-direction rather than an axial torque. The resulting shaft radial offset stiffness was calculated from the dividing the resulting reaction force by the displacement amount, according the standard method of DIN-740-Part2; the resulting misalignment stiffness is depicted in Table 4.8.

Table 4.8: Shaft parallel misalignment stiffness

Misalignment Type	Stiffness
	3.50×10^5 in-lb/in

Although the full coupling model is useful for mode, torsional, and parametric studies is useful for a coupling design engineer, this level of simulation detail is not as practical for a system designer. As discussed previously, a full power system is simplified to a series of stiffness and/or damping elements. Thus, a full numerical coupling model contradicts the relative simplicity of the power system analytical method. The next section will discuss a Reduced Order Modeling method that uses ANSYS to simplify the ANSYS numerical model.

5. Reduced-order Model of a Torsional Disk Coupling System

5.1. Model-order Reduction Approach

The design of an entire power system involves many components. Engineers may find it useful to analyze the flexible coupling itself in detail but it is impractical to use the full coupling model in conjunction with an entire system model; every bolt and disc pack would increase the complexity of the analysis. Thus, the reduced order modeling (ROM) technique can provide a means of directly simplifying the relatively complex full coupling model into a single element to be used in further analysis.

The reduction of order can be performed in ANSYS utilizing the existing coupling model used previously in modal and torsional stiffness studies. There are multiple steps involved in the simplification of the model using ANSYS [56] documented in Figure 5.1.

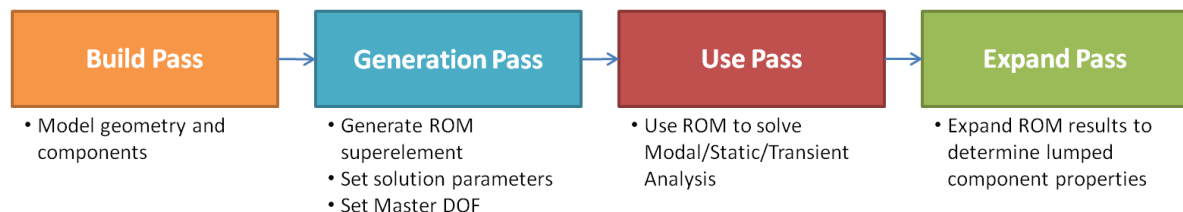


Figure 5.1: ANSYS ROM procedure

First is the Build Pass in which the coupling to be converted into a reduced order model is built in ANSYS. The next is the Generation Pass which uses a superelement method in ANSYS called Component Mode Synthesis (CMS). Typical applications of CMS use in ANSYS include aircraft or nuclear reactor analysis [56]. More generally, studies of large, complicated structures where design teams each engineer individual

components of the structure. Design changes to a single component affect only that component with additional computations only necessary for the modified subcomponent.

The Generation pass is used to set CMS parameters such as master degrees of freedom and the number of mode shapes to be used for superelement generation. In this case, the model is constrained at each rigid end of which a load or constraint would be applied to the coupling. ANSYS considers this as a fixed-interface case and the rigid end selections acts as the master degrees of freedom; see Figure 5.2.

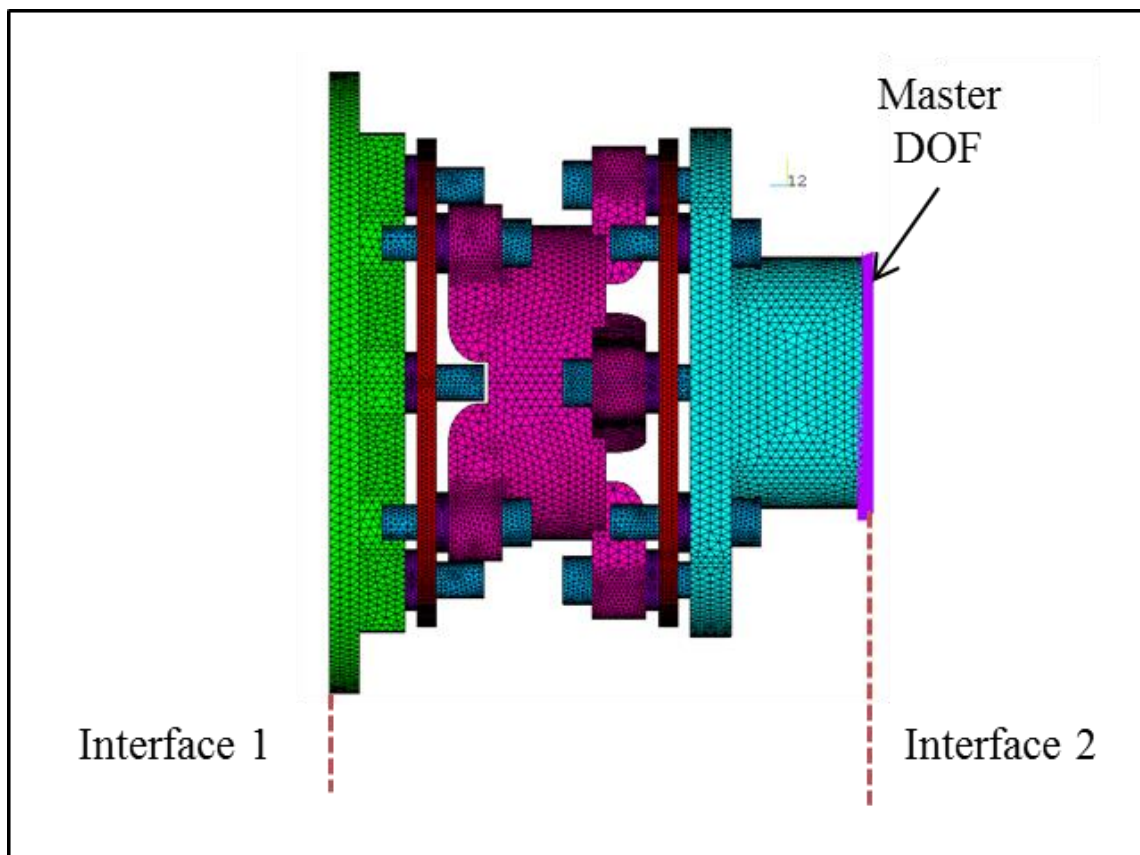


Figure 5.2: ROM model Master DOF

Another parameter is used as the number of modes extracted from the component to be used in superelement generation; this value was set to 10 modes. Also, it is

important to set the analysis type as *substructuring* or 'substr' in ANSYS with an extraction of the mass and stiffness matrix from the part of interest. CMS employs the Block Lanczos eigensolution method when using modes in the generation pass. The Use Pass utilizes the full model and previously created superelement simultaneously during modal analysis. Finally, the Expansion Pass interprets the results of from the superelement analysis allowing for the depiction of results corresponding to each mode.

5.2. Results

The resulting solution after modal analysis can be used to study the stresses and deformed shape of the component; see figure as an example. Mode #7, the bending of the coupling, exhibits highest stresses on the flexible disc component of the coupling.

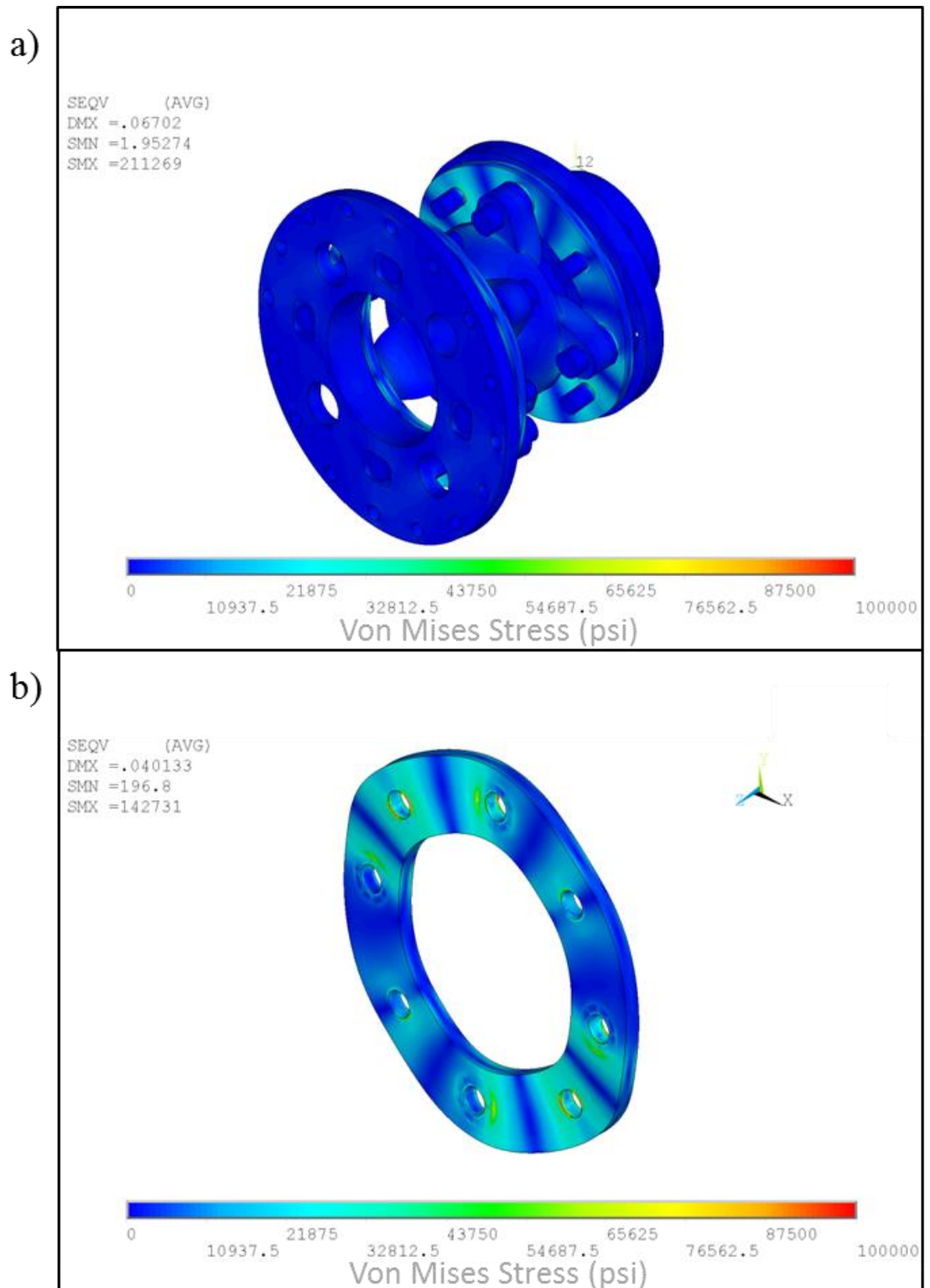


Figure 5.3: ROM mode #7 stress contour a) entire coupling b) isolated disc pack

Through this ROM process, various types of simulations may be conducted; see Figure 5.4. The ROM modal analysis results can be used to interpret stress in the deformed mode states. Also, an applied torque can be used to analyze various displacement angles quickly, similar to the torsional stiffness study.

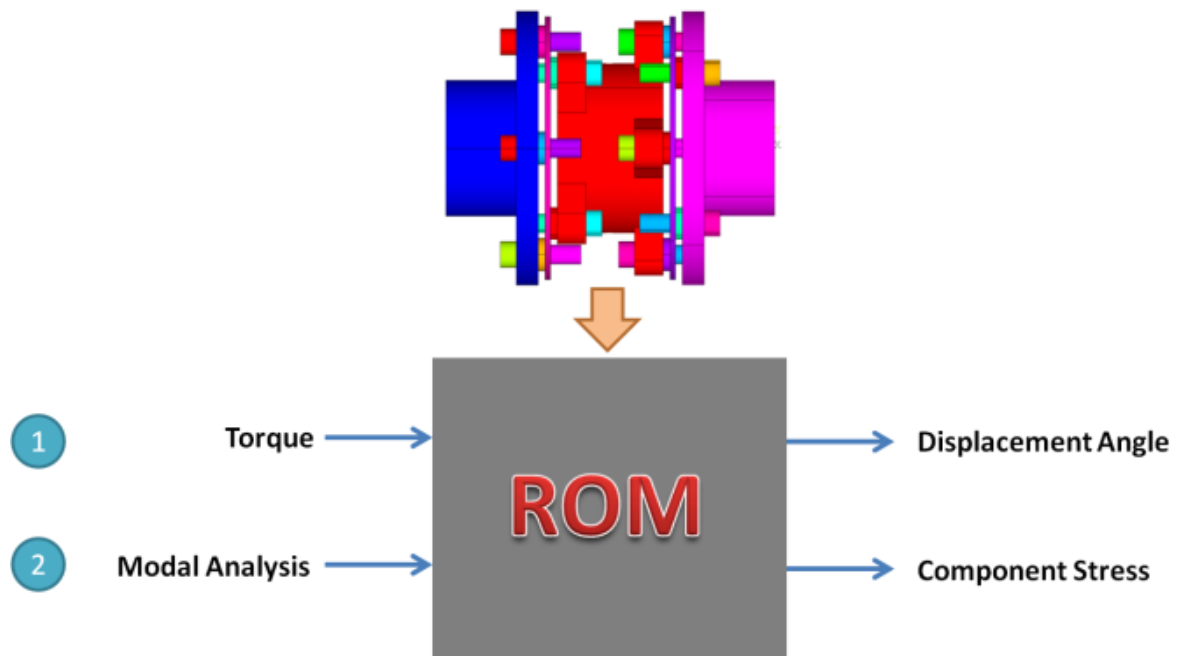


Figure 5.4: ROM superelement example capabilities

6. Experimental Validation

6.1. Experimental Setup and Results

In order to benchmark the ANSYS finite element results, experimental manufacturer data was used for comparison. The experimental procedure of constraints and loads are identical to that of the ANSYS simulations. The flywheel adapter is constrained to a rigid base-plate using all available bolt holes. The load is applied to an input shaft as an incremental torque. Experimental data was taken with digital indicators monitoring the relative angular deflection between input shaft and the fixed rigid support with individual component indicators as well; see Figure 6.1 or indicator placements.

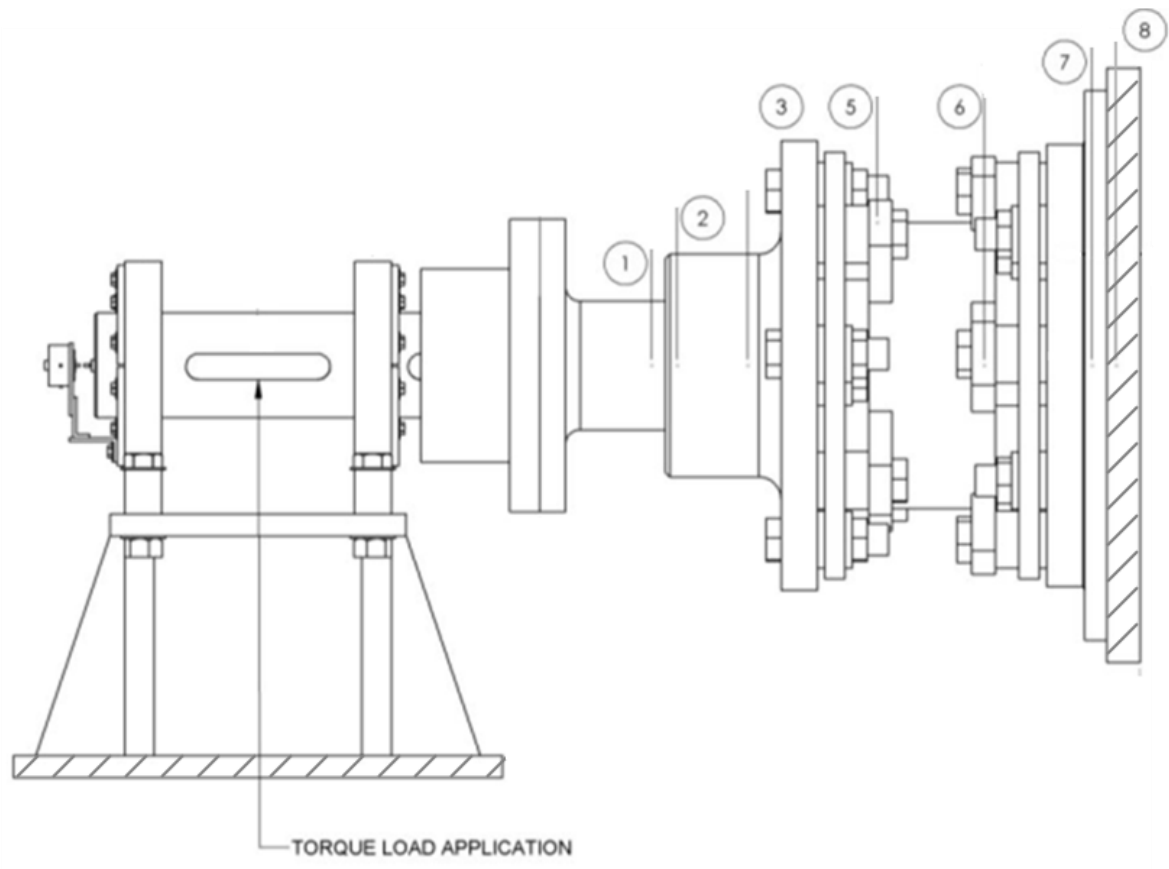


Figure 6.1: Experimental Set-up and Indicator Placements [Rexnord]

The torsional stiffness of the coupling is calculated with reference to the torsional windup (compliance) between indicators #1-#8 relative to the maximum input torque of 1.5 M-in-lb specific to this study. The following equations for torsional windup, Eqn. 6.1, and torsional stiffness, Eqn. 6.2, are shown as follows:

$$\varphi_T = \frac{[|A_8|+|A_1|]}{T_{max}} \quad (6.1)$$

where:

φ_T = Torsional windup (rad/in-lb)

A_8 = Absolute value of rotation angle at Indicator #8 relative to hub (rad)

A_1 = Absolute value of rotation angle at Indicator #1 relative to hub (rad)

T_{max} = Maximum applied torque (in-lb)

$$K_T = \frac{1}{\varphi_T} \quad (6.2)$$

where:

K_T = Torsional stiffness (in-lb/rad)

After interpreting the results of the experimental study, the torsional stiffness of this specific coupling was determined to be 6.67×10^8 in-lb/rad. This value is calculated using the torsional windup from indicators #1 - #8. As discussed in Section 4, there are two methods used in ANSYS to determine coupling torsional stiffness. The first, Method 1, pertains to the torsional windup between indicator #1 - #8 and Method 2 uses the torsional windup value calculated from the indicators connected directly to the coupling ends, indicator #2 - #7. A summary of the experimental results and comparison to the ANSYS simulation results is shown in Table 6.1. In comparison, the ANSYS simulation results are within 10% of the experimental results using both methods of torsional stiffness interpretation. Specifically, the results using torsional windup between

indicators #1 - #8 are 9.22% higher in the ANSYS simulation. Similarly, using the torsional windup from indicators #2 - #7, the ANSYS results are only 3.00% higher than the experimental results.

Table 6.1: Comparison of simulation results with experimental results

Indicator	#1 - #8		#2 - #7	
	Experimental	ANSYS	Experimental	ANSYS
K_T (in-lb/rad)	6.67×10^8	7.28×10^8	10.4×10^8	10.7×10^8
Δ	9.22%		3.00%	

6.2. Comparison of Analytical, Reduced-order and Full Models

With 90% accuracy between the ANSYS and experimental data, another study was conducted to verify the accuracy of the ANSYS method of calculating torsional stiffness. A theoretical shaft analytical calculation is compared to the same numerical calculations conducted in the ANSYS environment.

A theoretical cylindrical shaft with one end fixed and a torque applied to the other follows the general torsional stiffness equation is as shown in Eqn. #6-3 [65], [71].

Given an example stainless steel shaft with parameter detailed in Table 6.2, the torsional stiffness value equates to 14,126 in-lb/rad.

$$K_T = \frac{GJ}{L} \quad (6.3)$$

$$\text{with: } G = \frac{E}{2(1+\nu)}, \quad J = \frac{\pi d^4}{32}$$

where:

G = Shear Modulus

J = Second Moment of Inertia
 L = Length of shaft
 E = Elastic Modulus
 ν = Poisson's Ratio
 d = diameter of shaft

Table 6.2: Theoretical shaft parameters

Parameter	Value	Units
E_{steel}	2.97E+07	psi
ν	0.29	-
G	1.15E+07	psi
J	0.01	in ⁴
d	0.5	in
l	5	in

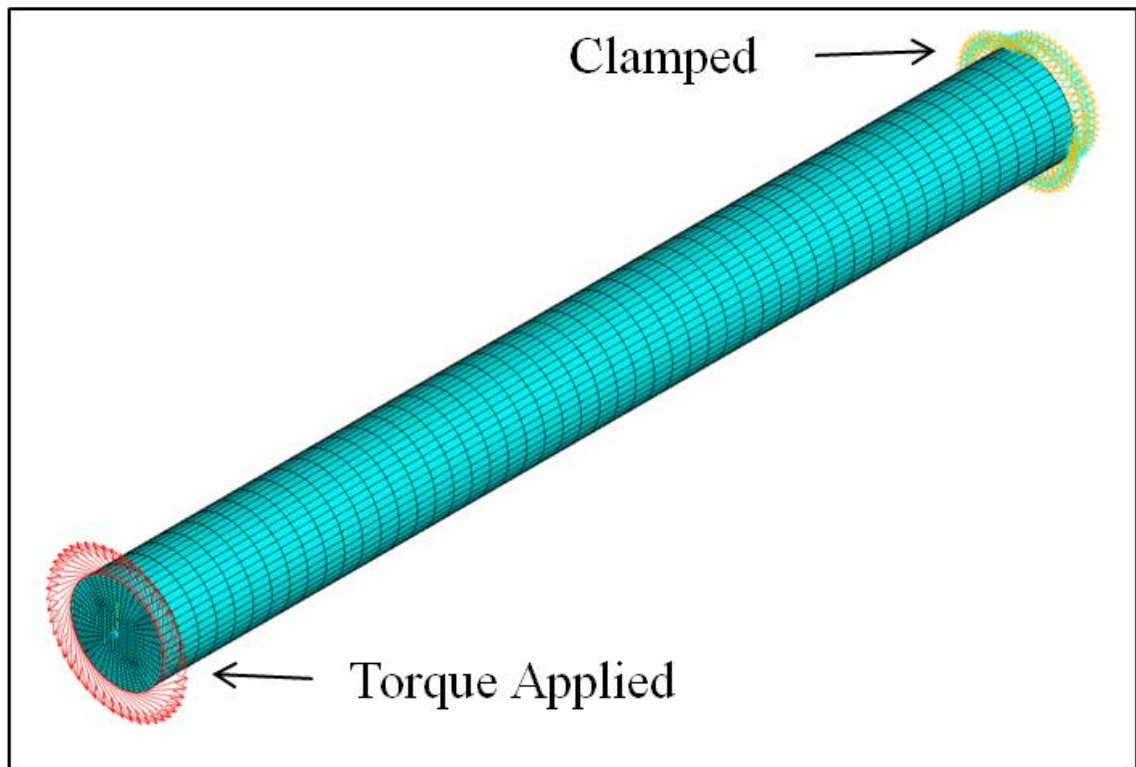


Figure 6.2: Simulated shaft constraints and loads

Now, in comparison with ANSYS, the same shaft is modeled with identical constraints and loading; Figure 6.2. Interpreting the results of the simulation yield a torsional stiffness value of 14,039 which in regards to the previous theoretical calculations is 99% accurate; Table #6-3. Since the ANSYS method and result interpretation has been verified it can be concluded that the coupling simulation results are also accurate. Thus, the comparison of experimental results and simulation results depicted in Table 6.3 holds true.

Table 6.3: Comparison of theoretical and simulation shaft results

Parameter	Value (in-lbs/rad)	Accuracy
$K_{T,theory}$	14,126	99%
$K_{T,ANSYS}$	14,039	

7. Summary of Results

7.1. Conclusions

A useful tool for flexible coupling designers and power system engineers alike has been successfully developed with avenues for continuing research and development. The torsional stiffness of a flexible disc coupling was studied experimentally by an industry manufacturer and numerically using the ANSYS environment. The ANSYS model proved effective for analyzing the torsional stiffness of the coupling with 90% accuracy and above relative to the experimental data. Not only did the study prove useful for torsional stiffness interpretation, but for other studies as well. Additional studies such as misalignment stiffness, reduced order modeling, and modal analysis have been briefly covered with promising initial results. The methods of theoretical calculation of industry coupling torsional stiffness remain undetermined with a comparative accuracy to ANSYS results of 38%.

The shear studies of the disc pack using a Timoshenko-beam approach produced inconclusive results. At the moment, the difference between multiple disc and solid disc pack shear modulus is negligible, justifying the use of a solid disc pack in the larger full coupling model used throughout this study. However, since the numerical values of shear modulus are approximately 30% from the theoretical value for steel, further investigation is needed to accurately derive the response of the full multi-layer disc pack.

The use of reduced-order modeling was successful for deriving stress distributions according to mode shape deformations, but this method has a broad impact on system modeling techniques. Reduced-order modeling can be implemented at various stages of

the design process; such as during entire power system design or additional disc pack analysis.

7.2. Contributions

This study provides insight into advanced methods for flexible disc coupling design. Industry data and recommendation can become more accurate by the use and expansion of the methods detailed in this study. These methods can be used in effort to minimize the difference between operational coupling response and the properties proposed by the designer, helping reduce power system failure, down time and energy consumption.

The developed procedure for reduced order modeling in this study can immediately be used to create a coupling element in a full system simulation. Future procedures for superelement creation would best be implemented after a coupling design change. The change of design or coupling type would result in a change of mass or stiffness properties for use in a system simulation. Reduced order modeling is the connection between a detailed coupling model and a simplified full system model. Also, another application for ROM is during coupling design. For example, if the flexible element of the coupling model becomes increasingly complex (i.e. multiple non-linear disc contacts) the disc pack component can initially be isolated and studied individually with a superelement created from the results then implemented in the full coupling model.

7.3. Future Work

The avenues opened by this study lead to a deeper understanding of power system design from the ability to study individual components of a flexible coupling or the implications a coupling has on the entire system. Individual component studies for further analysis include a continuation of disc pack modeling using contact pairs between every disc to establish a means of quantifying effective disc pack properties. These properties then can be used in an updated coupling model with non-linear material properties. With this representation of the assembly, a conclusion even more accurate than the current study may be determined.

Also, additional work characterizing the misalignment stiffness the remaining modes of misalignment can be conducted with implications towards power system modeling. Similarly, the creation of a reduced order modeling procedure for the full coupling provides options of continued research.

As a parametric model, the proposed methods can be applied to the remainder of the comparable product line from the current manufacturer; eventually even to different types of flexible disc coupling products. Each coupling model can be converted into a reduced order model using the proposed methods and employed in a full system model. This provides an increase comfort for customers to know that the coupling to be used in their system will perform as designed.

REFERENCES

- [1] R. L. Mott, *Machine Elements in Mechanical Design*. New York: Macmillan Publishing Company, 1992, pp. 354–355.
- [2] Rexnord, “Rexnord® Couplings – Reciprocating Compressors.” Rexnord Industries LLC., 2008.
- [3] Rexnord, “Rexnord and Falk – The Gold Standard in the Mining Industry.” Rexnord Industries LLC.
- [4] B. E. Thomas, “Flexible Coupling,” 2,182,711, 1957.
- [5] Huco, “A Designer’s Guide to Precision Shaft Couplers,” 1992.
- [6] J. A. Collins, *Mechanical Design of Machine Elements and Machines*. John Wiley & Sons, Inc., 2003, pp. 341–343.
- [7] LoveJoy, “Sorting Out Flexible Couplings.”
- [8] I. Redmond and K. Al-Hussain, “Misalignment as a Source of Vibration in Rotating Shaft Systems,” *19th Int. Modal Anal. Conf.*, pp. 118–123, 2001.
- [9] R. E. Munyon, J. R. Mancuso, and C. B. Gibbons, “The Application of Flexible Couplings for Turbomachinery,” *Proc. 18th Turbomach. Symp.*, pp. 1–25, 1989.
- [10] J. R. Mancuso, *Couplings and Joints*, 2nd ed. New York: Marcel Dekker, Inc., 1999.
- [11] J. R. Mancuso, “General Purpose vs Special Purpose Couplings,” *Proc. 23rd Turbomach. Symp.*, pp. 167–177.
- [12] J. R. Mancuso, J. Zilbeman, J. P. Corcoran, and K. P. T. Products, “Flexible-element couplings: How safe is safe?,” *Rotating Equip.*, no. December, pp. 93–96, 1994.
- [13] J. Corcoran, D. Lyle, P. McCormack, and T. Ortel, “Advances In Gas Turbine Couplings,” *Proc. 36th Turbomach. Symp.*, pp. 157–72, 2007.
- [14] Gam, “Testing Coupling Torsional Stiffness to Maximize Servo Positioning Speed and Accuracy,” 1.1.
- [15] E. I. Rivin, *Stiffness and Damping in Mechanical Design*. New York: Marcel Dekker, Inc., 1999.
- [16] M. P. Boyce, *Gas Turbine Engineering Handbook*, 4th ed. Elsevier, 2012.

- [17] R. L. Bielawa, "Drive System Dynamics," in *Rotary Wing Structural Dynamics and Aeroelasticity*, American Institute of Aeronautics and Astronautics, 1992, pp. 133–161.
- [18] M. L. Adams, *Rotating Machinery Vibration From Analysis to Troubleshooting*. New York: Marcel Dekker, Inc., 2001.
- [19] J. Vance, F. Zeidan, and B. Murphy, "Torsional vibration," in *Machinery Vibration and Rotordynamics*, Hoboken, New Jersey: John Wiley & Sons, Inc., 2010, pp. 35–70.
- [20] D. Dobre, S. Ionel, A. Victor Gabriel, A. George Mihail, and P. Nicoleta, "Finite Element Analysis of the Flexible Coupling With Metallic Membranes," *Proc. 21st Int. DAAAM Symp.*, vol. 21, no. 1, pp. 421–423, 2010.
- [21] D. Ray, "A Study on FEA of Torsional Vibration in Geared Shafts," National Institute of Technology Rourkela, 2010.
- [22] F. E. Rheume, H. Champiaud, and L. Zhaoheng, "On The Computing of the Torsional Rigidity of a Harmonic Drive Using FEA," in *International ANSYS Conference*, 2006.
- [23] C.-Y. Tsai and S.-C. Huang, "Transfer matrix for rotor coupler with parallel misalignment," *J. Mech. Sci. Technol.*, vol. 23, no. 5, pp. 1383–1395, May 2009.
- [24] F. R. Szenasi and W. von Nimitz, "Transient Analyses of Synchronous Motor Trains," *Proc. 7th Turbomach. Symp.*, pp. 111–117.
- [25] H. S. Jia, S. B. Chun, and C. W. Lee, "Evaluation of The Longitudinal Coupled Vibrations in Rotating , Flexible Disks/ Spindle Systems," *J. Sound Vib.*, vol. 208, no. 2, pp. 175–187, 1997.
- [26] R. E. Mondy and J. Mirro, "The Calculation and Verification of Torsional Natural Frequencies for Turbomachinery Equipment Strings," *Proc. 11th Turbomach. Symp.*, pp. 151–156.
- [27] T. Feese and C. Hill, "Guidelines for Preventing Torsional Vibration Problems in Reciprocating Machinery," in *Gas Machinery Conference*, 2002.
- [28] T. Feese and R. Maxfield, "Torsional Vibration Problem with Motor/ID Fan System Due to PWM Variable Frequency Drive," in *Proceedings of the 37th Turbomachinery Symposium*, 2008, pp. 45–56.
- [29] J. C. Wachel and F. R. Szenasi, "Analysis of Torsional Vibrations in Rotating Machinery," *Proc. 22nd Turbomach. Symp.*, pp. 127–151.
- [30] T. Kiekbusch, D. Sappok, B. Sauer, and I. Howard, "Calculation of the Combined Torsional Mesh Stiffness of Spur Gears with Two- and Three-Dimensional Parametrical FE Models," *Strojniški Vestn. – J. Mech. Eng.*, vol. 57, no. 11, pp. 810–818, Nov. 2011.
- [31] M. C. Cevik, M. Rebbert, and F. Maassen, "A New Approach for Prediction of Crankshaft Stiffness and Stress Concentration Factors," pp. 1–20, 2010.

- [32] M. M. Calistrat and G.G. Leaseburge, "Torsional Stiffness of Interference Fit Connections," *Mech. Conf. Int. Symp. Gearing Transm.*, pp. 1–8, 1973.
- [33] S. M. Sheikh, "Analysis of Universal Coupling Under Different Torque Condition," *Int. J. Eng. Sci. Adv. Technol.*, vol. 2, no. 3, pp. 690–694, 2012.
- [34] A. Kahraman, H. N. Ozguven, D. R. Houser, and J. J. Zakrajsek, "Dynamic Analysis of Geared Rotors by Finite Elements," 102349, 1990.
- [35] D. Dobre and S. Ionel, "Design of Elastic Couplings with Metallic Flexible Membranes," *Proc. 1st Int. Conf. Manuf. Eng.*, vol. I, no. Volume I, pp. 51–56.
- [36] R. D. A. Ovalle, "An Analysis of the Impact of Flexible Coupling Misalignment on Rotordynamics," Texas A&M University, 2010.
- [37] C. B. Gibbons, "Coupling Misalignment Forces," *Proc. 5th Turbomach. Symp.*, pp. 111–116.
- [38] A. W. Lees, "Misalignment in rigidly coupled rotors," *J. Sound Vib.*, vol. 305, no. 1–2, pp. 261–271, Aug. 2007.
- [39] A. Askarian and S. M. R. Hashemi, "Effect of Axial force, Unbalance and Coupling Misalignment on Vibration of Rotor Gas Turbine," *14th Int. Congr. Sound Vib.*, 2007.
- [40] A. Khatkhate, S. Gupta, A. Ray, and R. Patankar, "Anomaly detection in flexible mechanical couplings via symbolic time series analysis," *J. Sound Vib.*, vol. 311, no. 3–5, pp. 608–622, Apr. 2008.
- [41] A. T. Tadeo and K. L. Cavalca, "A Comparison of Flexible Coupling Models for Updating in Rotating Machinery Response," *J. Brazilian Soc. Mech. Sci. Eng.*, vol. 25, no. 3, pp. 235–246, 2003.
- [42] C. de Villemagne and R. E. Skelton, "Model reductions using a projection formulation," *Int. J. Control*, vol. 46, no. 6, pp. 2141–2169, 1987.
- [43] Z. Bai, "Krylov subspace techniques for reduced-order modeling of large-scale dynamical systems," *Appl. Numer. Math.*, vol. 43, no. 1–2, pp. 9–44, Oct. 2002.
- [44] M.-T. Yang and J. H. Griffin, "A Reduced-Order Model of Mistuning Using a Subset of Nominal System Modes," *J. Eng. Gas Turbines Power*, vol. 123, no. 4, p. 893, 2001.
- [45] R. W. Freund, "Krylov-subspace methods for reduced-order modeling in circuit simulation," *J. Comput. Appl. Math.*, vol. 123, no. 1–2, pp. 395–421, Nov. 2000.
- [46] A. C. Antoulas and D. C. Sorensen, "Approximation of large-scale dynamical systems: An overview," *Technical Report*, vol. 1892. Electrical and Computer Engineering, Rice University, Houston, TX, pp. 1–22, 2001.

- [47] I. Avdeev and M. Shams, "Vascular stents: Coupling full 3-D with reduced-order structural models," *IOP Conf. Ser. Mater. Sci. Eng.*, vol. 10, pp. 1–9, Jun. 2010.
- [48] C. Gu, "Model Order Reduction of Nonlinear Dynamical Systems," UCB/EECS-2012-217, 2012.
- [49] A. Saito and B. I. Epureanu, "Bilinear modal representations for reduced-order modeling of localized piecewise-linear oscillators," *J. Sound Vib.*, vol. 330, no. 14, pp. 3442–3457, Jul. 2011.
- [50] J. Burkardt, Q. Du, M. Gunzburger, and H.-C. Lee, "Reduced order modeling of complex systems," in *NA03 Dundee*, 2003, pp. 29–38.
- [51] V. Ganine, D. Laxalde, H. Michalska, and C. Pierre, "Parameterized reduced order modeling of misaligned stacked disks rotor assemblies," *J. Sound Vib.*, vol. 330, no. 3, pp. 445–460, Jan. 2011.
- [52] M. Itoh, "Vibration suppression control for a dies-driving spindle of a form rolling machine: Effects of a model-based control with a rotational speed sensor II," in *Proceedings of the 2009 IEEE International Conference on Mechatronics and Automation*, 2009, pp. 3827–3832.
- [53] K. D'Souza and A. Saito, "Reduced Order Modeling for Nonlinear Vibration Analysis of Mistuned Multi-Stage Bladed Disks with a Cracked Blade," in *52nd AIAA/ASME/ASCE/AHS/ASC Structures, Structural Dynamics and Materials Conference*, 2011, no. April.
- [54] M. Byrtus, "Dynamic Analysis of Reduced Order Large Rotating Vibro-Impact Systems," *Int. J. Mech. , Ind. Sci. Eng.*, vol. 7, no. 11, pp. 1263–1270, 2013.
- [55] B. O. Al-Bedoor and a. a. Al-Qaisia, "Stability analysis of rotating blade bending vibration due to torsional excitation," *J. Sound Vib.*, vol. 282, no. 3–5, pp. 1065–1083, Apr. 2005.
- [56] "ANSYS Theory Manual. Release 14.0." SAS IP, Inc, 2011.
- [57] J. E. Mehner, L. D. Gabbay, and S. D. Senturia, "Computer –Aided Generation of Nonlinear Reduced-Order Dynamic Macromodels-II: Stress-Stiffened Case." .
- [58] J. E. Mehner and F. Vogel, "Coupled Electro-Elastic Domain Solver and ROM Extractor for MEMS." .
- [59] ANSI/AGMA-9004-B08, "Flexible Couplings -- Mass Elastic Properties and Other Characteristics," vol. 08. American Gear Manufacturers Association, 2008.
- [60] DIN-740-Part-2, "Power Transmission Engineering- Flexible Shaft Couplings Parameters and Design Principles." DIN, 1986.

- [61] W. D. Callister and D. G. Rethwisch, *Materials Science and Engineering: An Introduction, 8th Edition*, 8th ed. United States of America: John Wiley & Sons, Inc., 2010.
- [62] MatWeb, “Overview of materials for Medium Carbon Steel.” p. 1, 2014.
- [63] MatWeb, “Overview of materials for Cast Iron.” pp. 1–2, 2014.
- [64] Matbase, “GS-45 cast steel alloy,” vol. 3. 2014.
- [65] T. A. Philpot, *Mechanics of Materials*, 2nd ed. John Wiley & Sons, Inc., 2011.
- [66] D. L. Logan, *A First Course in the Finite Element Method*, 5th ed. USA: Cengage Learning, 2012.
- [67] J. N. Reddy, *An Introduction to Nonlinear Finite Element Analysis*. USA: Oxford University Press, 2004.
- [68] M. A. Hili, T. Fakhfakh, and M. Haddar, “Failure analysis of a misaligned and unbalanced flexible rotor,” *J. Fail. Anal. Prev.*, vol. 6, no. 4, pp. 73–82, Aug. 2006.
- [69] D. Dobre, S. Ionel, A. Victor Gabriel, A. George Mihail, and D. Tiberiu, “Failure Modes of Flexible Metallic Membrane Couplings,” *Proc. 21st Int. DAAAM Symp.*, vol. 21, no. 1, pp. 419–421, 2010.
- [70] J. P. Corcoran, J. A. Kocur, and M. C. Mitsingas, “Preventing Undetected Train Torsional Oscillations,” *Proc. 39th Turbomach. Symp.*, pp. 135–146, 2010.
- [71] W. A. Tuplin, *Torsional Vibration*. Sir Isaac Pitman and Sons Ltd., 1966.